

ESCUELA TÉCNICA SUPERIOR DE INGENIEROS
INDUSTRIALES Y DE TELECOMUNICACIÓN

UNIVERSIDAD DE CANTABRIA



Trabajo Fin de Grado

**New composite photocatalysts with graphene for
the treatment of perfluorinated compounds**

(Nuevos fotocatalizadores compuestos con grafeno
aplicados al tratamiento de compuestos
perfluorados)

Para acceder al Título de

Graduado/a en ingeniería química

Autor: Belén García Merino

Julio-2018

I would like to express my gratitude for the help, time and dedication provided by my project directors, Ane Miren Urriaga and Beatriz Gómez Ruiz, during the development of this final degree project.

I would also like to acknowledge Project CTM2016-75509-R (MINECO – FEDER 2016-2020).

Finally, I wish to thank my family and friends for their support and encouragement during this work and throughout my studies.

INDEX

1. INTRODUCTION.....	1
1.1 Context.....	1
1.1.1 Characterization of Perfluoroalkyl substances.....	1
1.1.2 Sources and transport of perfluorooctanoic acid.....	2
1.1.3 Human exposure, adverse effects and legislation of PFOA.....	3
1.1.4 PFOA removal technologies.....	5
1.2 Objectives.....	7
2. EXPERIMENTAL PROCEDURE.....	7
2.1 Reagents.....	7
2.2 Synthesis of the compositeTiO ₂ -rGO.....	8
2.3 Medium pressure Hg lamp reactor.....	9
2.3.1 Experimental set-up.....	9
2.3.2 PFOA degradation experiments.....	9
2.4 LEDs lamp reactor.....	10
2.4.1 Experimental set-up.....	10
2.4.2 PFOA degradation experiments.....	10
2.4.3 Measurement of the formation of hydroxyl radicals.....	11
2.5 Analytical methods.....	11
2.6 Statistical treatment of the results.....	12
3. RESULTS AND ANALYSIS.....	12
3.1. Characterization of TiO ₂ -rGO composite.....	12
3.3. LEDs reactor.....	17
3.3.1 Time delay study.....	20
4. CONCLUSIONS.....	25
5. REFERENCES.....	26
6. ANNEXES.....	31

6.1 ANNEX I: Medium pressure Hg lamp reactor	31
3.4 ANNEX II: LEDs lamp reactor	33
3.5 ANNEX III: Time delay study	35

LIST OF FIGURES

Figure 1. PFOA molecular structure	2
Figure 2. PFOA transport (Post et al, 2007).....	3
Figure 3. Formation of e ⁻ and h ⁺ when absorbing UV light (Nakata and Fujishima, 2012)	6
Figure 4. (A) Photocatalytic experimental setup showing medium pressure Hg lamp reactor and thermostating bath (B) Hg lamp.....	9
Figure 5. (A) Photocatalytic setup with LEDs lamp reactor and (B) PVC case inside showing the LEDs strips and glass reactor	10
Figure 6. ATR-FTIR spectra of GO, TiO ₂ and TiO ₂ -rGO	13
Figure 7. (A) PFOA degradation, (B) fluoride release and (C) PFOA mineralization, under different conditions, in a medium pressure Hg lamp reactor with an initial 0.24 mM PFOA concentration.....	14
Figure 8. (A) PFOA degradation, (B) Fluoride release, (C) PFCAs generation (during TiO ₂ -rGO photocatalytic treatment) and (D) TOC removal, under different conditions, in a LEDs lamp reactor with an initial 0.24 mM PFOA concentration.....	17
Figure 9. Irradiance emitted by LEDs lamp during 8 hours.	21
Figure 10. Generation of hydroxyl radicals applying photocatalysis with both 0.1 g ·L ⁻¹ TiO ₂ -rGO and 0.1 g ·L ⁻¹ TiO ₂ , with an initial 0.25 mol ·L ⁻¹ DMSO solution	21
Figure 11. Progress of (A) PFOA removal and (B) fluoride release under different conditions, using the composite TiO ₂ -rGO catalyst in a LEDs lamp reactor with an initial 0.24 mM PFOA concentration. Power to LEDS lamp = 75 W.	22
Figure 12. (A) PFOA degradation and (B) Fluoride release in photocatalytic experiments using TiO ₂ -rGO with different initial PFOA concentrations in a LEDs lamp reactor. Power to LEDS lamp = 75 W.	24
Figure 13. PFCAs formed in a medium pressure Hg lamp reactor with a 0.24mM Initial PFOA solution for (A) TiO ₂ catalyst and (B) TiO ₂ -rGO.....	31

Figure 14. Calculated and Measured TOC data in a medium pressure Hg lamp reactor with a 0.24 mM initial PFOA solution for (A) direct photolysis (B) photocatalysis with TiO ₂ and (C) photocatalysis with TiO ₂ -rGO.....	32
Figure 15. Fluorine mass balance and fluoride release in a LEDs lamp reactor reactor with a 0.24 mM initial PFOA solution for (A) direct photolysis (B) photocatalysis with TiO ₂ and (C) photocatalysis with TiO ₂ -rGO.....	33
Figure 16. Calculated and measured TOC in a LEDs lamp reactor reactor with a 0.24 mM initial PFOA solution for (A) direct photolysis (B) photocatalysis with TiO ₂ and (C) photocatalysis with TiO ₂ -rGO	34
Figure 17. Formation of (A) PFHpA, (B) PFPxA, (C) PFPeA and (D) PFBA in photocatalytic experiments, under different conditions, using TiO ₂ -rGO with a 0.24mM initial PFOA concentration in a LEDs lamp reactor. Power to the LEDS lamp = 75W.	35
Figure 18. TOC trends in photocatalytic experiments, under different conditions, using TiO ₂ -rGO with a 0.24mM initial PFOA concentration in a LEDs lamp reactor. Power to the LEDS lamp = 75W.	36
Figure 19. TOC trends in photocatalytic experiments, under different conditions, using TiO ₂ -rGO in a LEDs lamp reactor. Power to the LEDS lamp = 75W.	36

LIST OF TABLES

Table 1. PFOA physical-chemical properties (Adapted from Fuji et al, 2007).....	2
Table 2. PFOA degradation and TOC removal percentages, and final fluoride release concentrations in photolysis, photocatalysis with TiO ₂ and photocatalysis with TiO ₂ -rGO catalyst.	15
Table 3. Figured out hypothesis and planned experimental strategies.....	20

ABSTRACT

Poly- and Perfluoroalkyl substances (PFASs) are a group of anthropogenic pollutants, which have been widely used in industry manufacturing and as part of consumer products due to their unique physicochemical properties. However, their persistence, global distribution and bio-accumulation have resulted in the increasing concern of the regulatory bodies, particularly for perfluorooctanoic acid (PFOA) which was highly produced and emitted to the environment (Fuertes et al, 2017; Squadrone et al, 2015; Urtiaga et al, 2015) . Moreover, the inherent resistance of PFASs to most conventional water treatments makes necessary to investigate clean and effective technologies for the treatment of PFASs at sources of emissions and polluted waters (Domínguez et al, 2016; Soriano et al, 2017; Urtiaga et al, 2018).

The present final degree project has as main objective the study of the degradation of PFOA using the advanced oxidation process: heterogeneous photocatalysis. For this purpose, a bibliographic research about PFASs characteristics and distribution in the environment and photocatalysis application to PFOA degradation has been performed. After that, experimental work was carried out to investigate the degradation of PFOA using a prepared photocatalyst based on TiO₂ nanoparticles and reduced graphene, synthesized using a hydrothermal method as a promising strategy to overcome the limitations of TiO₂.

The photocatalytic experiments were carried out in two different systems. The experiments carried out in a batch reactor provided with a medium pressure Hg lamp, resulted in similar PFOA removal rates by means of direct photolysis and photocatalysis with the use of TiO₂ and the prepared TiO₂-rGO composite. Moreover, these findings were different compared to the previous reported work under similar experimental conditions (Gómez-Ruiz et al, 2018), which likely showed the instability of the Hg lamp. The experiments performed in a light emitting diodes (LEDs) batch reactor, showed that after 12 hours applying direct photolysis and TiO₂-mediated photocatalysis to a 0.24 mM PFOA solution, no degradation was observed. On the contrary, using 0.1 g · L⁻¹ of TiO₂-rGO catalyst, the near-complete PFOA removal (99 ± 1 %) was achieved. This effective photoactivity of the TiO₂-rGO composite catalyst could be attributable to the good properties of graphene that make it act as a trap of electrons, decreasing the high

electron/hole recombination of the TiO₂ semiconductor and promoting the electrons transfer, which favours the initial degradation steps of PFOA. (Wang et al, 2013; Wang et al, 2017; Gómez-Ruiz et al, 2018).

Moreover, the photocatalytic degradation of PFOA by means of TiO₂-rGO exhibited an initial time delay before any PFOA degradation could be observed, which was quantified in about two hours. Several tests were carried out in order to associate the delay with irradiation of LEDs, hydroxyl radicals generation, PFOA adsorption, TiO₂-rGO catalyst activation under UV light or limitations of mass transfer. However, among all the tests, only PFOA initial concentration influenced the photocatalytic process, noting that the higher it was, the faster the degradation took place.

Finally, relevant conclusions about the effectiveness of the TiO₂-rGO catalyst and the different photocatalytic systems have been obtained.

RESUMEN

Las sustancias poli- y perfluoroalquílicas (PFASs) son un grupo de contaminantes antropogénicos que han sido ampliamente usados en la industria manufacturera y como parte de productos de consumo debido a sus propiedades físico-químicas únicas. Sin embargo, su persistencia, distribución global y bio-acumulación han dado lugar a una creciente preocupación por parte de los cuerpos reguladores, particularmente hacia el ácido perfluorooctanoico (PFOA) que fue altamente producido y emitido al medioambiente (Fuertes et al, 2017; Squadrone et al, 2015; Urtiaga et al, 2015). Además, la resistencia inherente de los PFASs a la mayoría de los tratamientos de agua convencionales, hace necesario investigar tecnologías limpias y efectivas para el tratamiento de los PFASs en las fuentes de emisiones y las aguas contaminadas (Domínguez et al, 2016; Soriano et al, 2017; Urtiaga et al, 2018).

El presente trabajo de fin de grado tiene por objetivo principal el estudio de la degradación de PFOA mediante el proceso de oxidación avanzada: fotocátalisis heterogénea. Para ello, se ha realizado una búsqueda bibliográfica sobre las características y distribución de los PFASs en el medioambiente y la fotocátalisis aplicada a la degradación de PFOA. A continuación, se llevó a cabo un trabajo experimental para

investigar la degradación de PFOA utilizando un catalizador basado en nanopartículas de TiO_2 y grafeno reducido, que fue sintetizado utilizando un método hidrotermal como una estrategia prometedora para superar las limitaciones del TiO_2 .

Los experimentos fotocatalíticos se llevaron a cabo en dos sistemas diferentes. Los experimentos desarrollados en un reactor discontinuo provisto de una lámpara de Hg de presión media, resultaron en tasas de eliminación de PFOA similares al usar fotólisis directa y fotocátalisis con TiO_2 y con el compuesto TiO_2 -rGO preparado. Además, estos resultados fueron diferentes a los reportados anteriormente en otro trabajo bajo similares condiciones experimentales (Gómez-Ruiz et al, 2018), lo que probablemente se deba a una inestabilidad por parte de la lámpara de Hg. Los experimentos realizados en un reactor discontinuo de lámpara de LEDs, mostraron que después de 12 horas aplicando fotólisis directa y fotocátalisis con TiO_2 a una solución inicial de PFOA de 0.24 mM, no se observó degradación. Por el contrario, utilizando 0.1 g. L^{-1} de catalizador TiO_2 -rGO, se logró una eliminación de PFOA casi completa ($99 \pm 1 \%$). Esta efectiva fotoactividad del catalizador TiO_2 -rGO podría atribuirse a las buenas propiedades del grafeno que lo hacen actuar como un captor de electrones, disminuyendo la alta recombinación del par electrón/hueco del semiconductor TiO_2 y promoviendo la transferencia de electrones, la cual favorece los primeros pasos de la degradación de PFOA (Wang et al, 2013; Wang et al, 2017; Gómez-Ruiz et al, 2018).

Además, la degradación fotocatalítica de PFOA por medio de TiO_2 -rGO mostró un tiempo de retardo inicial, antes de que pudiera observarse degradación de PFOA, que se cuantificó en unas dos horas. Se realizaron varias pruebas para asociar el tiempo de retardo con: irradiación de los LEDs, generación de radicales hidroxilos, adsorción de PFOA, activación del catalizador TiO_2 -rGO bajo luz UV o limitaciones en la transferencia de masa. Sin embargo, de entre todas las pruebas desarrolladas, únicamente la concentración inicial de PFOA mostró una influencia en el proceso fotocatalítico, observándose que cuanto más alta era ésta, más rápida era la degradación.

Finalmente, se han obtenido conclusiones relevantes sobre la efectividad del catalizador TiO_2 -rGO y los diferentes sistemas fotocatalíticos.

1. INTRODUCTION

1.1 Context

1.1.1 Characterization of Perfluoroalkyl substances

Poly- and Perfluoroalkyl substances (PFASs) are a kind of emerging organic contaminants, classified as persistent organic pollutants (POPs). They contain fully fluorinated carbon alkyl chains of various lengths and a final functional group, being the carbon-fluorine bond responsible of PFASs properties such as thermal and chemical stability. Moreover, the combination of hydrophobicity from fluorinated structures and hydrophilicity from functional groups gives PFASs excellent surfactant performance.

All those characteristics make PFASs widely used since the early 1950s both in industrial manufacturing or as components of consumer products, for example, as reactants for polyurethane production and vinyl polymerization or as components of herbicides, insecticides, cosmetics, greases, paints, adhesives or aqueous film forming foams used for firefighting. However, their resistance to hydrolysis, photolysis and microbial degradation makes PFASs highly persistent and widespread in the environment, especially in water. (Bartlett and Davis, 2018; Lee J.W et al, 2017; Squadrone et al, 2015; Urtiaga et al, 2015; Fuertes et al, 2017).

PFASs include thousands of chemicals, although, perfluoroalkyl acids (PFAAs) are the most widely studied. These can be divided, according to their final functional group, into perfluoroalkyl carboxylic acids (PFCAs) or perfluoroalkyl sulfonic acids (PFSAs).

Perfluorooctanoic acid (PFOA) was one of the most commonly used PFAAs, and therefore is among the most widespread PFASs in the environment. It has the chemical formula $C_8F_{15}COOH$ and its chemical structure is shown in Figure 1, the high electronegativity of the fluorinated alkyl chain makes PFOA to be dissociated in aqueous solutions. Other properties are depicted in Table 1.

These properties make PFOA useful for many different applications. For example, it can be used as emulsifier, such as in the manufacturing of Teflon used for coating of cooking pans, as a surfactant such as soap or shampoo, and in galvanizing baths (Fuji et al, 2007).

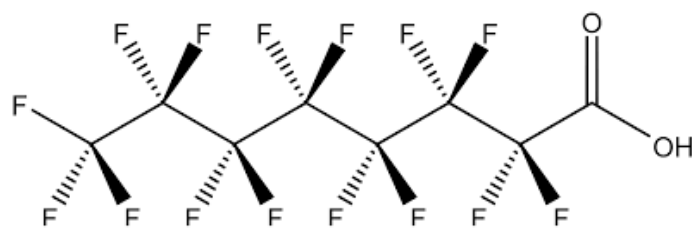


Figure 1. PFOA molecular structure

Table 1. PFOA physical-chemical properties (Adapted from Fuji et al, 2007).

Molecular weight	414 g · mol ⁻¹
Melting point	45-50 °C
Boiling point	189-192 °C
Density	17 g · cm ⁻³
Solubility in pure water	3.4 g · L ⁻¹
Vapour pressure (25°)	10 mm Hg

1.1.2 Sources and transport of perfluorooctanoic acid

Sources of PFCAs emissions to the environment can be classified as direct or indirect. The main direct PFOA contamination source is the manufacturing of ammonium perfluorooctanoate (APFO) and its subsequent use in fluoropolymer production. Besides, the majority of APFO (80-90%) is manufactured through the electrochemical fluorination process, while the remaining 10-20% of APFO is manufactured by direct oxidation of perfluorooctyl iodide.

Indirect sources are those where PFCAs are presented as chemical reaction impurities or when substances degrade to form PFCAs. Indirect PFOA sources only account for 10% of the total PFOA emissions. For example, fluorotelomer alcohols (FTOHs) and perfluorooctane sulfonyl fluoride (POSF) based chemicals can degrade to PFOA in the environment (Prevedouros et al, 2006; Pistocchi and Loos, 2009).

PFOA arrives to the environment mainly because of the industrial facilities, by emissions to the air or discharge into rivers. If PFOA is emitted to the atmosphere, it is able to deposit into soil and migrate through this soil until arriving to the groundwater. Once this contaminant arrives to groundwater, it may enter into water supply wells, as

described in Figure 2. Otherwise, if industries discharge PFOA into rivers, its polarity and mobility in water allow it to reach the sea and, consequently, this compound can be distributed globally.

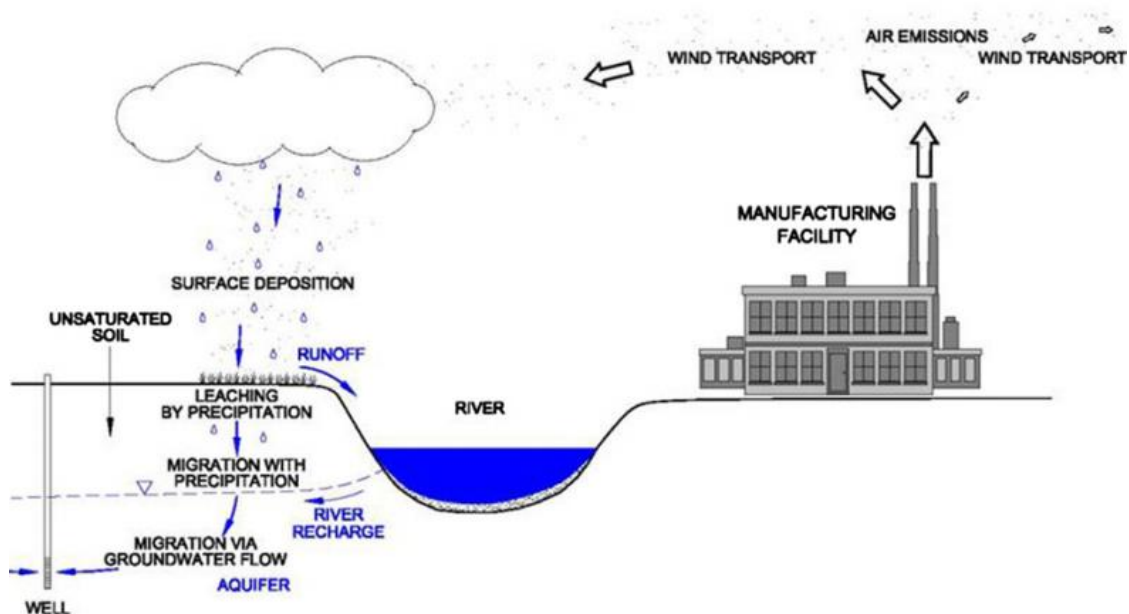


Figure 2. PFOA transport (Post et al, 2007).

Another possibility is that PFOA enters to groundwater or surface water from other sources different from industrial facilities. For example, by storm water runoff (Figure 2), release of aqueous firefighting foams, or within the waste water treatment plant (WWTP) effluents, although, in a WWTP, PFCAs can also be adsorbed into sewage sludge, which may be used for the land treatment or disposed on dump sites, leading to the remobilisation of these compounds (Hardkova et al, 2010; Post et al, 2007).

1.1.3 Human exposure, adverse effects and legislation of PFOA

Humans are exposed to PFOA through different pathways, for example, direct skin contact from impregnated products such as carpets or clothing, the inhalation of aerosols in consumer products or the high concentrations of PFOA at indoor air, outdoor air and dust. Nevertheless, the consumption of contaminated food or drinking water is considered the greatest source and the main pathway of human exposure to PFCAs like PFOA (Hardkova et al, 2010; Post et al, 2007).

PFOA can be taken up into plants grown on contaminated soil, including into vegetables and grains consumed by humans and livestock; it can be also eaten by edible fish and other seafood or migrate from wrappers into food, resulting in both cases in human consumption. Consequently, PFOA has been detected in several types of food, for instance, meats, fish, vegetables, milk, butter or microwave popcorn.

In Europe, typical adult exposures to PFOA are about $2\text{-}3\text{ ng}\cdot\text{kg}^{-1}\cdot\text{day}^{-1}$ and serum levels varies from $2\text{-}3.6\text{ ng}\cdot\text{mL}^{-1}$ according to a study performed with a sample of 200 adults in three different countries (Greece, Belgium, Italy). PFOA persists in humans with a half-life of several years, in contrast to other common organic pollutants in drinking water such as benzene, or methyl tertiary butyl ether (MTBE), which are much more rapidly excreted (Post et al, 2007).

PFOA causes several types of toxicity in experimental animals whereas human epidemiological studies have found associations with numerous health endpoints resulting from exposure, however, causality has not been proven. Those health endpoints are even worst in children or people working in contact with PFOA (Appleman et al, 2014; Post et al, 2007). Considering PFOA potential toxicity and the extent of its environmental distribution, it has started to be regulated by international bodies.

In May 2016, the U.S. Environmental protection agency (EPA) established a drinking water health advisory (HA) of $0.07\text{ }\mu\text{g}\cdot\text{L}^{-1}$ for PFOA, in order to protect from the short-term as well as to lifetime exposure scenarios. As PFOA and perfluorooctane sulfonate acid (PFOS) are based on similar developmental effects and are numerically identical, when they co-occur at the same time and location in a drinking water source, EPA recommends to compare the sum of the concentrations of both chemicals to the previously mentioned HA.

Additionally, PFOA has been added to the EPA's contaminant candidate list 3 of chemicals under consideration for future drinking water regulation in the U.S and to the EPA's unregulated contaminant monitoring rule 3 (UCMR 3) which needs monitoring by public water suppliers to provide data for further decision making. Moreover, USEPA science advisory board has recommended PFOA to be considered a likely human carcinogen (Appleman et al, 2014; Flores et al, 2013; U.S. EPA, 2016).

In Europe, PFOA is contemplated in the OSPAR list of chemicals for priority action and in the candidate list of substances of very high concern (SVHC). From July 2008, the European Food Safety Authority (EFSA) has established for PFOA a tolerable daily intake equal to $1500 \text{ ng} \cdot \text{kg}^{-1} \text{ body weight}$ (Hradkova et al, 2010).

1.1.4 PFOA removal technologies

The scientific community is facing the challenge of developing clean technologies for the treatment at source of emissions of PFASs and for the abatement of the existing water polluted sites. Processes based on membranes, adsorption or ion exchange could be used, however, these technologies imply the transfer of the contaminants to a second phase and the generated waste must be managed (Urriaga et al, 2015).

During last decades, advanced oxidation processes (AOPs) have been taking more importance. They are effective technologies for degrading organic compounds, based on the generation of strongly reactive species such as hydroxyl radicals ($\cdot\text{OH}$). Among all the AOPs, this final degree project will focus on heterogeneous photocatalysis, which is a promising technology because of its ambient operating temperature and pressure and its absence of secondary pollution. Moreover, it could be solar driven so it is considered a sustainable technology (Domínguez et al, 2016; Soriano et al, 2017; Gómez-Ruiz et al, 2017; Urriaga et al, 2018).

Heterogeneous photocatalysis consist in the acceleration of a chemical reaction by the presence of a catalyst and light. The catalyst is usually a semiconductor, which has an orbital with an electronic band structure. In heterogeneous photocatalysis, there are two bands describing the range of energies that the electron has, one is the valence band (V_B) while the other is the conduction band (C_B). Between them, there is a band gap. When light of equal or greater energy than the one of the band gap is applied to semiconductors, an electron moves from the V_B (leaving a positive hole h^+) to the C_B (leaving an electron e^-). Then, both the h^+ and the e^- may migrate to the catalyst surface as described in Figure 3 (Haque et al, 2012; Nakata and Fujishima, 2012).

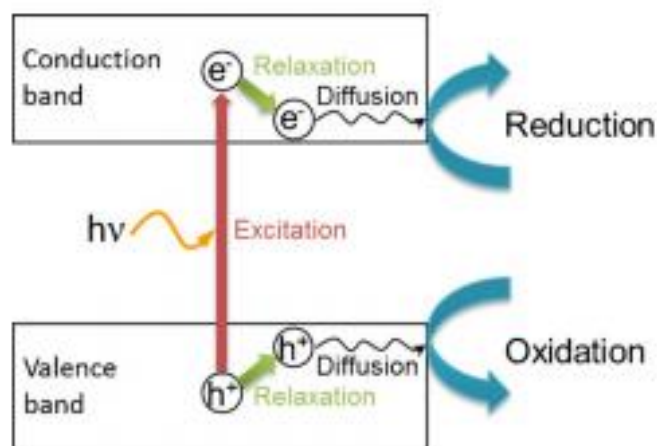


Figure 3. Formation of e^- and h^+ when absorbing UV light (Nakata and Fujishima, 2012)

Since 1980s, TiO_2 is the most commonly used catalyst for the treatment of organic matter, due to its non-toxicity, high efficiency at room temperature, easy availability, low cost, biological and chemical inertness and stability to photo and chemical corrosion. Once the formed electron and hole migrate to the surface of the TiO_2 , h^+ may react with water to produce hydroxyl radicals whereas e^- is picked up by oxygen to generate superoxide radical anion (O_2^-), these are the primary oxidizing species in the photocatalytic oxidation processes (Haque et al, 2012).

However, having a band gap of 3.2 eV, pure TiO_2 is only able to absorb and use radiation below 387 nm, corresponding mainly to the ultraviolet light (3-5% of the solar energy) and recombination of electron-hole pairs is also a problem. TiO_2 can be combined with carbon or silica materials in order to reduce the photo-generated electron-hole recombination rate and improve the photocatalytic properties of TiO_2 . Graphene is an allotrope of carbon, it is also one of the most promising materials to have a better photocatalytic activity and stability because of its excellent electrical and thermal properties, and its high specific surface area (Li et al, 2013b). For this reasons, efficiency of the TiO_2 -rGO catalyst for the removal of PFOA will be evaluated in this final degree project.

There is a large number of studies in which photocatalytic experiments are carried out with artificial light using conventional Hg or Xe lamps. Those lamps have some disadvantages as the short lifetimes and the low efficiency converting energy into light,

transforming photocatalysis in an energy intensive process, which is a key issue for the scale up and industrial implementation of the technology. Light Emitting Diodes (LEDs) appear as an alternative to the traditional light sources, because of their less toxic nature, higher energy efficiency, stability, durability and compact size (Domínguez et al, 2016).

In this final degree project, experiments will be carried out in both a medium pressure Hg lamp reactor and in a reactor provided with LEDs lamps, being the first research work that studies PFOA degradation using LEDs lamps and the composite TiO₂-rGO catalyst.

1.2 Objectives

The present final degree project has been carried out in the Chemical and Biomolecular Engineering Department of the University of Cantabria.

The aim of this project is to contribute to the study of the degradation of perfluorooctanoic acid by heterogeneous photocatalysis, studying different catalysts and light sources. For this purpose, the following objectives are defined:

1. Synthesis and characterization of the photocatalytic material, composed of TiO₂ and reduced graphene oxide (rGO).
2. PFOA photocatalytic degradation experiments with TiO₂-rGO and TiO₂ using a medium pressure Hg lamp.
3. PFOA photocatalytic degradation experiments with TiO₂-rGO and TiO₂, using LEDs lamps.
4. Analysis, comparison and evaluation of the experimental results.

2. EXPERIMENTAL PROCEDURE

2.1 Reagents

All chemicals were used as received without further purification and all solutions were prepared with ultrapure water (Q-POD Milipore). Graphite powder was obtained from Acros Organics. Sulfuric acid (H₂SO₄, 95%), sodium nitrate (NaNO₃), potassium permanganate (KMnO₄), chloride acid (37%), sodium di-hydrogen phosphate anhydrous

(NaH_2PO_4) and pH 4.0 H_3PO_4 - NaH_2PO_4 buffer solution were purchased from Panreac. Hydrogen peroxide (H_2O_2 , 30% v/v), dimethyl sulfoxide, ammonium acetate ($\text{CH}_3\text{COONH}_4$) and methanol (UHPLC-MS) were provided by Scharlau. TiO_2 (P25, 20% rutile and 80% anatase, $50 \text{ m}^2\cdot\text{g}^{-1}$, 21 nm) was supplied by Evonik Degussa. PFOA (96% purity) was provided by Sigma Aldrich chemicals. Finally, 2,4-dinitrophenylhydrazine was obtained from Aldrich.

2.2 Synthesis of the composite TiO_2 -rGO

The elaboration of the TiO_2 -rGO catalyst lies in two parts, following a procedure previously reported (Ribao et al, 2017; Li et al, 2013). The first one, is the synthesis of graphene oxide (GO) following the modified Hummers method (Hummers and Hoffman, 1958). This initial step consists on the oxidation of graphite by means of H_2SO_4 , NaNO_3 and KMnO_4 . Once the graphite was oxidized, the solution was centrifuged and washed with HCl to eliminate the NaNO_3 and H_2SO_4 in excess. This cleaning processes was repeated with UP water. After that, the graphite oxide (3D) was sonicated to obtain GO nanosheets (2D). The solid obtained was washed and centrifuged, in order to separate the solid part (graphite oxide) from the liquid part (graphene oxide and water). Finally, the GO was dried in an oven at $50 \text{ }^\circ\text{C}$ overnight (Pei et al, 2013).

The second part of the composite elaboration is the attachment of the GO nanosheets with TiO_2 nanoparticles using a hydrothermal procedure (Zhang y Pan, 2010). The most effective ratio of GO- TiO_2 is 5%-95% according to previous studies (Ribao et al, 2017). Based on this relation, 0.038 g of graphene oxide were weighted and added to UP water and the GO solution was sonicated for 1 h. Then, commercial TiO_2 (0.762 g) was added into the GO solution. After stirring for 2 h, this mixture was introduced in a 200 mL teflon-lined auto-clave and maintained at $120 \text{ }^\circ\text{C}$ for 3 h, to obtain simultaneously the reduction of oxygenated groups of the GO and the bonding with the TiO_2 . The TiO_2 -rGO obtained was centrifuged, washed with UP water and finally, dried in the oven at $50 \text{ }^\circ\text{C}$ for 12 hours (Li y cols, 2013b).

The prepared TiO₂-rGO composite was characterized by Attenuated total reflectance - Fourier transform infrared (ATR-FTIR) spectra recorded on a Spectrum Two spectrometer (Perkin Elmer).

2.3 Medium pressure Hg lamp reactor

2.3.1 Experimental set-up

Figures 4(A) and 4(B) show the experimental set-up. It consists of an 800 mL reactor, in which there is a 150 W medium pressure Hg lamp with a quartz cover (Heraeus Noblelight TQ 150 Z1). The emission wavelength of the lamp ranges between 200 and 600 nm. The system also has a thermostating bath (PolyScience) provided with a refrigerant fluid of water/ethylene glycol to achieve a temperature equal to 20°C inside the reactor, and a magnetic stirring plate (Agimatic-S, JP Selecta) to provide proper mixing to the solution during the experiments.

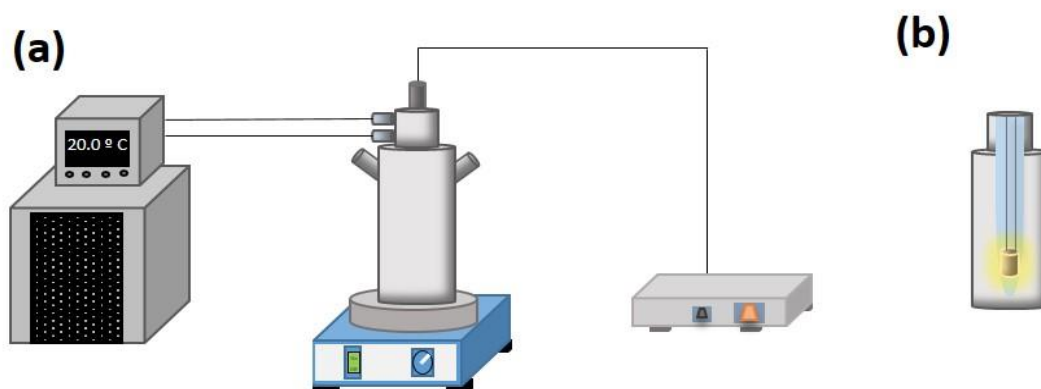


Figure 4. (A) Photocatalytic experimental setup showing medium pressure Hg lamp reactor and thermostating bath (B) Hg lamp

2.3.2 PFOA degradation experiments

First of all, the lamp and cooling system were switched on and, after 30 minutes of stabilization, 800 mL of PFOA solution (0.24 mmol·L⁻¹) were introduced in the reactor.

Initially, experiments only using UV light were performed to prove the efficacy of direct photolysis. Then, UV/catalyst experiments were performed, introducing the PFOA solution with 0.1 g·L⁻¹ of catalysts (TiO₂ or TiO₂-rGO). The concentration of catalyst was selected from previous studies (Gomez-Ruiz et al, 2017). Aliquots of 25 mL were sampled

at defined time intervals and, in the case of photocatalysis, filtered through 0.45 polypropylene filters prior to analysis.

2.4 LEDs lamp reactor

2.4.1 Experimental set-up

This experimental setup, shown in Figures 5(A) and 5(B), is an Apria Systems laboratory UV reactor. It consists of a dark PVC case (height 415 mm, diameter 210 mm), in which there is a Pyrex glass cylindrical reactor of 1 L of capacity (height=250 mm, diameter=74 mm) and 180 LEDs (LZ1-00UV00 LED ENGIN). The emission wavelength of each LED is 365 nm, they are assembled into 10 strips of 18 units, arranged uniformly in the angular direction of the case and separated 1.5 cm from the solution to be treated. The electric power of the system can be fixed at any value between 1 and 75 W. Finally, the system includes a magnetic stirring plate (Velp Scientifica) to provide proper mixing to the solution during the experiments.

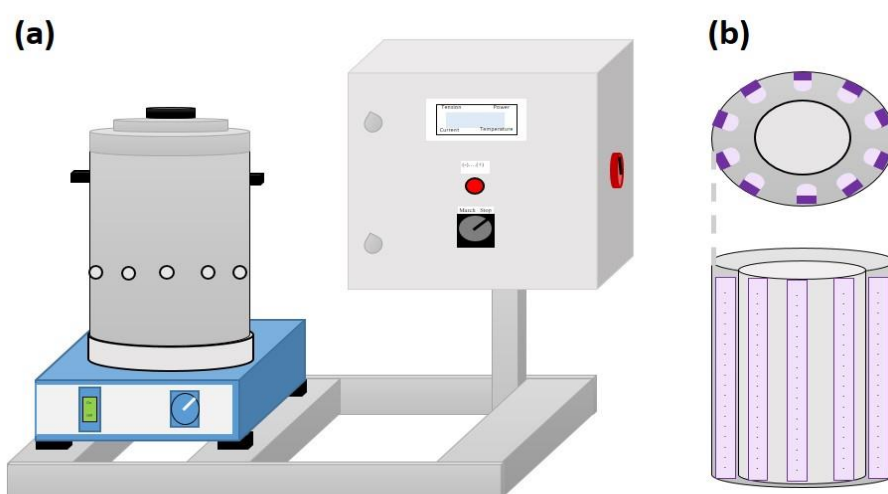


Figure 5. (A) Photocatalytic setup with LEDs lamp reactor and (B) PVC case inside showing the LEDs strips and glass reactor

2.4.2 PFOA degradation experiments

Firstly, photolysis was performed introducing 1 L of PFOA solution ($0.24\text{mmol} \cdot \text{L}^{-1}$) in the reactor and switching the light on. Power to the lamps was set at two values, 25 W and 75W. Aliquots of 25 mL were sampled at defined time intervals.

Finally, photocatalysis was performed introducing 1 L of PFOA solution with $0.1 \text{ g} \cdot \text{L}^{-1}$ of catalysts (TiO_2 or $\text{TiO}_2\text{-rGO}$), and establishing 75 W of light. Again, 25 mL of sample were taken at defined time intervals and filtered through 0.45 propylene filters prior to analysis. Additionally, the radiation emitted by the light source was measured using a photoradiometer HD 2102.1 (Delta OHM) during photocatalysis experiments.

2.4.3 Measurement of the formation of hydroxyl radicals

The formation of hydroxyl radicals can be indirectly measured using a method based on the reaction between $\cdot\text{OH}$ and DMSO to produce formaldehyde, which reacts with DNPH to form the corresponding hydrazine (DNPHo). The rate of $\cdot\text{OH}$ generation is considered the same as the rate of DMSO transformation into formaldehyde, which can be measured by analysing DNPHo by means of high performance liquid chromatography coupled to DAD UV-Vis detection (HPLC-DAD) (Tai et al, 2004).

To do so, 1L of a $0.25 \text{ mol} \cdot \text{L}^{-1}$ DMSO solution was mixed with $0.1 \text{ g} \cdot \text{L}^{-1}$ of composite $\text{TiO}_2\text{-rGO}$ catalyst and introduced in the reactor. Once the lamp was switched on, sample aliquots of 2 mL were taken at defined time intervals and filtered through 0.45 polypropylene filters. Then, 2.5 mL of buffer solution, 200 μL of DVPH and 300 μL of UP water were added to the sample, and the mixture was maintained at room temperature for 30 minutes before analysing it. This experiment was repeated with TiO_2 for comparison.

2.5 Analytical methods

In this final degree project, four different analytical methods were used.

First of all, a HPLC-DAD system (Waters 2695) equipped with an X-Bridge C18 column ($5\mu\text{m}$, $250 \text{ nm} \times 4.6 \text{ mm}$, Waters) was used for the measurement of DNPHo. The mobile phase was a mixture of methanol/ NaH_2PO_4 (65:35, v/v) with a flow rate of $0.5 \text{ mL} \cdot \text{min}^{-1}$. The retention time of the different compounds was identified by comparison with the previously injected standards.

Then, a HPLC-MS/MS (Acquity, Waters) and the X-Bridge BEH C18 (2.5 μm , 2.1 \times 75 mm) column were used to measure the concentration of PFOA, perfluoroheptanoic acid (PFHpA), perfluorohexanoic acid (PFHxA), perfluoropentanoic acid (PFPeA) and perfluorobutanoic acid (PFBA). The eluents were pure methanol and an aqueous solution containing H_3COONH_4 2 $\text{mmol} \cdot \text{L}^{-1}$ and 5% of methanol. The eluent flow rate was 0.15 $\text{mL} \cdot \text{min}^{-1}$. The limit quantification (LOQ) for each compound was 1 $\mu\text{g} \cdot \text{L}^{-1}$.

Furthermore, fluoride concentration was measured using ion chromatography (ICS-1100, Dionex) equipped with an ion exchange resins column (AS9-HC, Dionex) and a conductivity detector with suppressor device. Na_2CO_3 (9 mM) was used as mobile phase.

Finally, total carbon (TC) and inorganic carbon (IC) were measured by TOC-V CPH (Shimadzu) using a calibration curve that established relationship between the area under the peak of the CO_2 signal of the sample and its concentration. The total organic carbon (TOC) was obtained as the difference between TC and IC.

2.6 Statistical treatment of the results

In certain cases, experiments have been carried out twice so that reproducibility could be proven. Those results are shown as mean values \pm standard deviation.

Additionally, data obtained with the Hg medium pressure lamp reactor were analysed using the student's t-test method ($p < 0.05$). That method is a statistic tool incorporated in Excel, used for comparing the difference between two means in relation to the variation in the data, expressed as the standard deviation of the difference between means.

3. RESULTS AND ANALYSIS

3.1. Characterization of TiO_2 -rGO composite

Figure 6 shows the FTIR spectrum of the TiO_2 -rGO composite, in order to evaluate the correct preparation of the photocatalyst. Moreover, FTIR spectra of TiO_2 and GO were also represented for comparison.

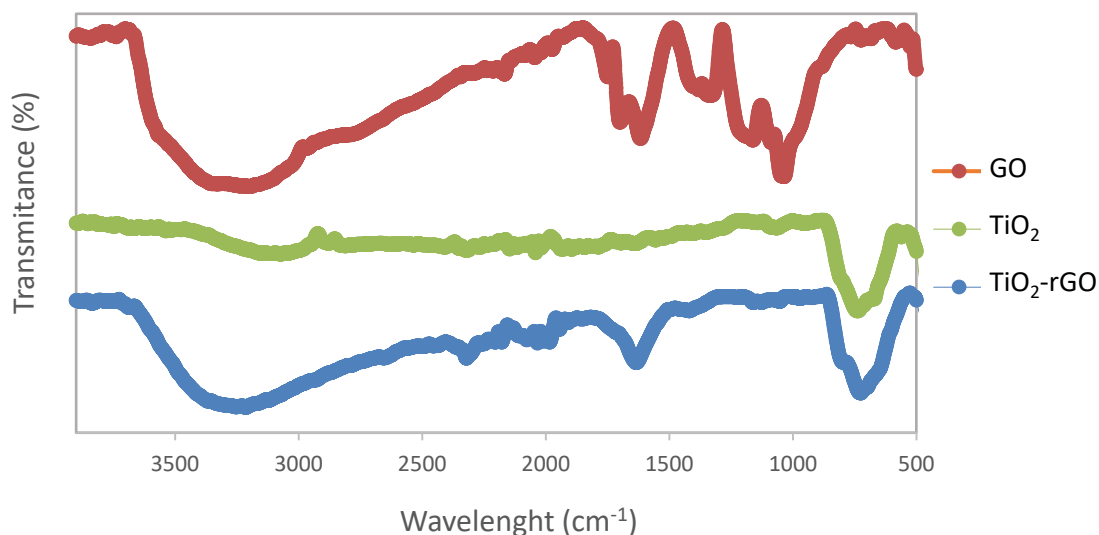


Figure 6. ATR-FTIR spectra of GO, TiO₂ and TiO₂-rGO

On the one hand, GO spectrum showed strong absorption peaks corresponding to various oxygen functional groups: water –OH (3400-3100 cm⁻¹), carboxylates or ketones C=O (1694 cm⁻¹), water –OH or C=C (1614 cm⁻¹), alcohol group C-OH (1400 cm⁻¹), epoxide C-O-C or phenolic C-O-H (1160 cm⁻¹) and alcoxy C-O (1032 cm⁻¹). On the other hand, the FTIR results of TiO₂ showed an absorption peak at 550-850 cm⁻¹, which is attributed to the stretching vibration of Ti-O-Ti bonds.

After the hydrothermal treatment, the composite TiO₂-rGO still showed the peaks corresponding to –OH and C=C, while the intensity of the peaks corresponding to other oxygen functional groups (C=O, C-OH, C-O-C, C-O-H and C-O) had decreased significantly, meaning that the GO was significantly reduced. Furthermore, this spectrum exhibited an increase in the intensity of the peak at 550-850 cm⁻¹ representing the presence of Ti-O-C bonds in addition to the Ti-O-Ti ones (Wang et al, 2013).

3.2. Photocatalytic decomposition of PFOA

3.2.1 Medium pressure Hg lamp reactor

Firstly, the removal of PFOA by direct photolysis under UV irradiation was studied. Then, the photocatalytic degradation using the commercial TiO₂ and the composite TiO₂-rGO

catalyst was evaluated. Samples were taken at defined time intervals and analyzed with the analytical methods. The results obtained are represented in Figures 7 to 9.

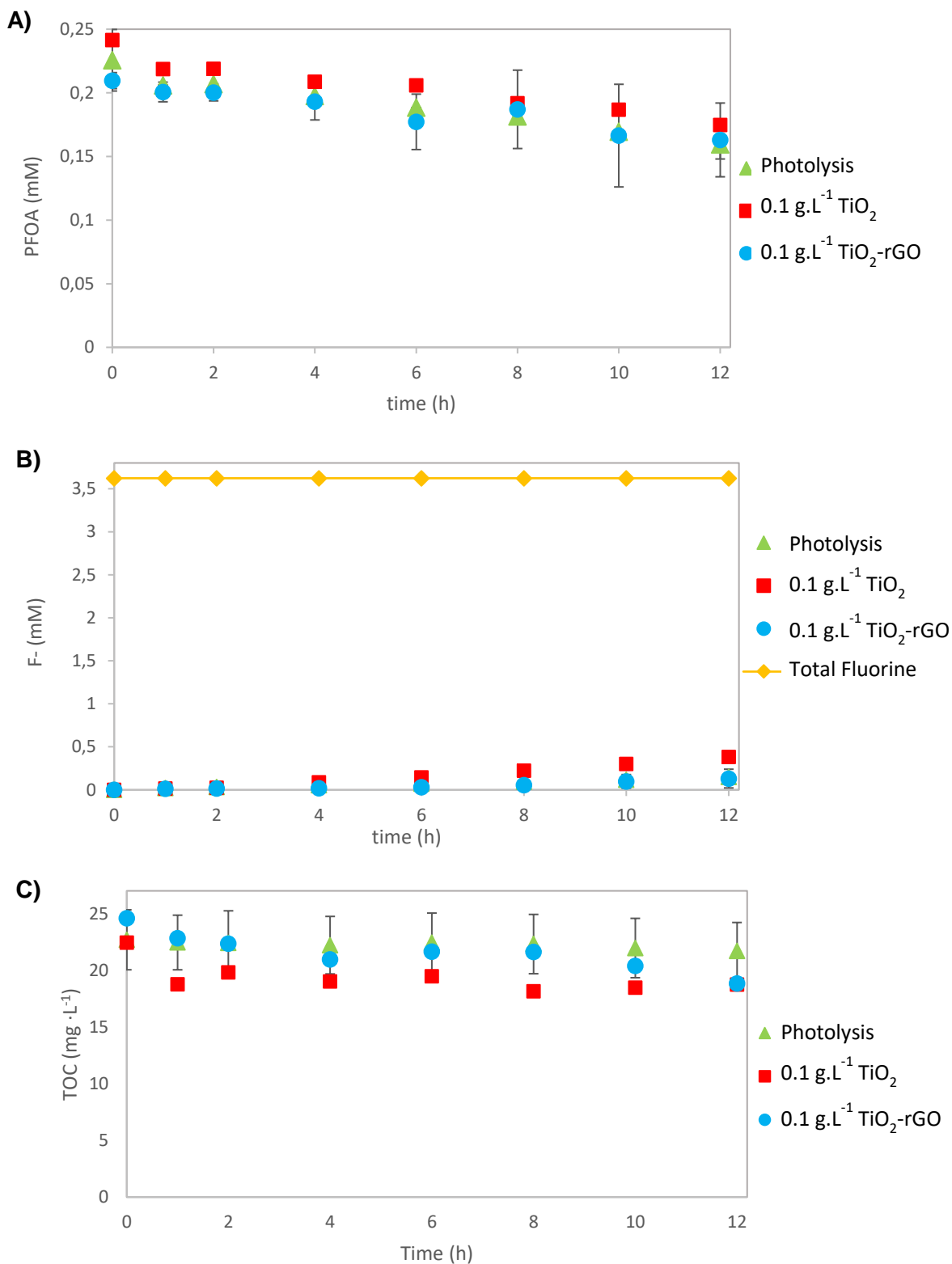


Figure 7. (A) PFOA degradation, (B) fluoride release and (C) PFOA mineralization, under different conditions, in a medium pressure Hg lamp reactor with an initial 0.24 mM PFOA concentration.

Additionally, PFOA degradation and TOC removal percentages, and final fluoride release concentrations at the end of the three treatments are shown in Table 2. In the case of photocatalysis with TiO₂-rGO there are no average values and deviances for TOC removal due to a problem with the analytical equipment.

Table 2. PFOA degradation and TOC removal percentages, and final fluoride release concentrations in photolysis, photocatalysis with TiO₂ and photocatalysis with TiO₂-rGO catalyst.

	Photolysis	Photocatalysis 0.1 g · L⁻¹ TiO₂	Photocatalysis 0.1 g · L⁻¹ TiO₂-rGO
PFOA degradation ratio	29 ± 4 %	28%	27 ± 11 %
TOC removal	4 ± 3 %	16%	23 %
Fluoride release	0.15 mM	0.38 mM	0.13 mM

Figure 7(A) shows PFOA concentration measured within 12 hours during the previously mentioned experiments. Low PFOA degradation ratios were obtained in all cases, with values in the range of 27-29%. Based on these results, two conclusions can be reached. The first one is that the results were not fully reproducible, according to the high deviation observed in TiO₂-rGO experiments. Secondly, it could not be known whether any process was more effective than the others, because the degradation percentages were not significantly different according to the student's t-test performed. In contrast, previous work on PFOA photocatalytic degradation developed under the same experimental conditions resulted in different findings (Gomez-Ruiz et al., 2018). The authors reported that PFOA degradation rates were 58 ± 9 % for direct photolysis, 24 ± 11% for photocatalysis with TiO₂ and 93 ± 7 % for photocatalysis with TiO₂-rGO catalyst. These differences between the reported data and the results shown in the present work (Table 2) can be attributable to the performance of the Hg lamp. Even though the standard stabilization time of Hg lamp was carried out, it seems that the stabilization of the lamp was not achieved during this work.

Figure 7(B) shows the concentration of the fluoride released during 12 hours of PFOA treatments, and also, the fluorine content corresponding to the initial PFOA concentration. Fluoride was released by the cleavage of the C-F bond in the alkyl chains of those molecules. According to data shown in Table 2, the final fluoride concentrations in the solution were 0.15 mM by direct photolysis, 0.38 mM by photocatalysis with TiO₂,

and 0.13 mM with the TiO₂-rGO photocatalyst. Those concentrations were considered insignificant when compared with the total fluorine forming part of the initial PFOA solution (3.62 mM), proving the low PFOA degradation in all the experiments. Particularly, the higher fluoride content during the TiO₂-mediated process can be attributable to an experimental error in the analytic technique, or to the problem of instability of the lamp.

Additionally, the generation of shorter-chain PFCAs in the photocatalytic experiments was monitored. They are formed as intermediates when PFOA degrades, following a stepwise degradation mechanism that consist of PFOA losing one –CF₂ group to give PFHpA as the first degradation product, and consecutively PFHxA, PFPeA and PFBA. Shorter-chain PFCAs are volatile and cannot be measured in the aqueous samples. Results obtained are detailed in Figure 13, ANNEX I. As it can be observed, the concentration of PFHpA, as the first degradation product, was higher compared to the shorter-chain PFCAs. However, these concentrations of intermediate products were very low, in accordance to the poor PFOA degradation ratio.

Besides, PFOA mineralization was studied by means of measuring the evolution of TOC. Figure 7(C) showed the change of TOC with the irradiation time during the 12 hours of treatments. The TOC progress represents the conversion of organic carbon from contaminant molecules into CO₂. The TOC removal ratios were slower than the corresponding PFOA degradation in all cases, as shown in Table 2. This is in agreement with the step-by-step degradation pathways of PFOA to form intermediate products before the complete mineralization (Gómez-Ruiz et al, 2018).

Moreover, the progress of TOC concentration was calculated from the carbon atoms in the PFOA and intermediates molecules quantitatively analysed (Figure 14, ANNEX 1). It is remarkable that the calculated TOC for direct photolysis and photocatalysis with TiO₂-rGO were slightly lower than the measured values. Additionally, to prove the effect of the presence of F⁻ in the solution on TOC measurements, three samples of 10 mg.L⁻¹, 20 mg.L⁻¹ and 50 mg.L⁻¹ of NaF were prepared and measured. The results obtained were 1.36 mg.L⁻¹, 1.62 mg.L⁻¹ and 0.44 mg.L⁻¹ respectively, showing the analytical error associated to the TOC analysis of these types of samples which contributed to the gap between calculated and measured TOC in Figure 14.

3.3. LEDs reactor

Experiments were aimed at evaluating PFOA degradation by direct photolysis, and photocatalysis by means of TiO_2 and the prepared TiO_2 -rGO catalysts under LEDs irradiation. The progress of PFOA and intermediate PFCAs concentrations, fluoride ions released and TOC removal are shown in Figures 8.

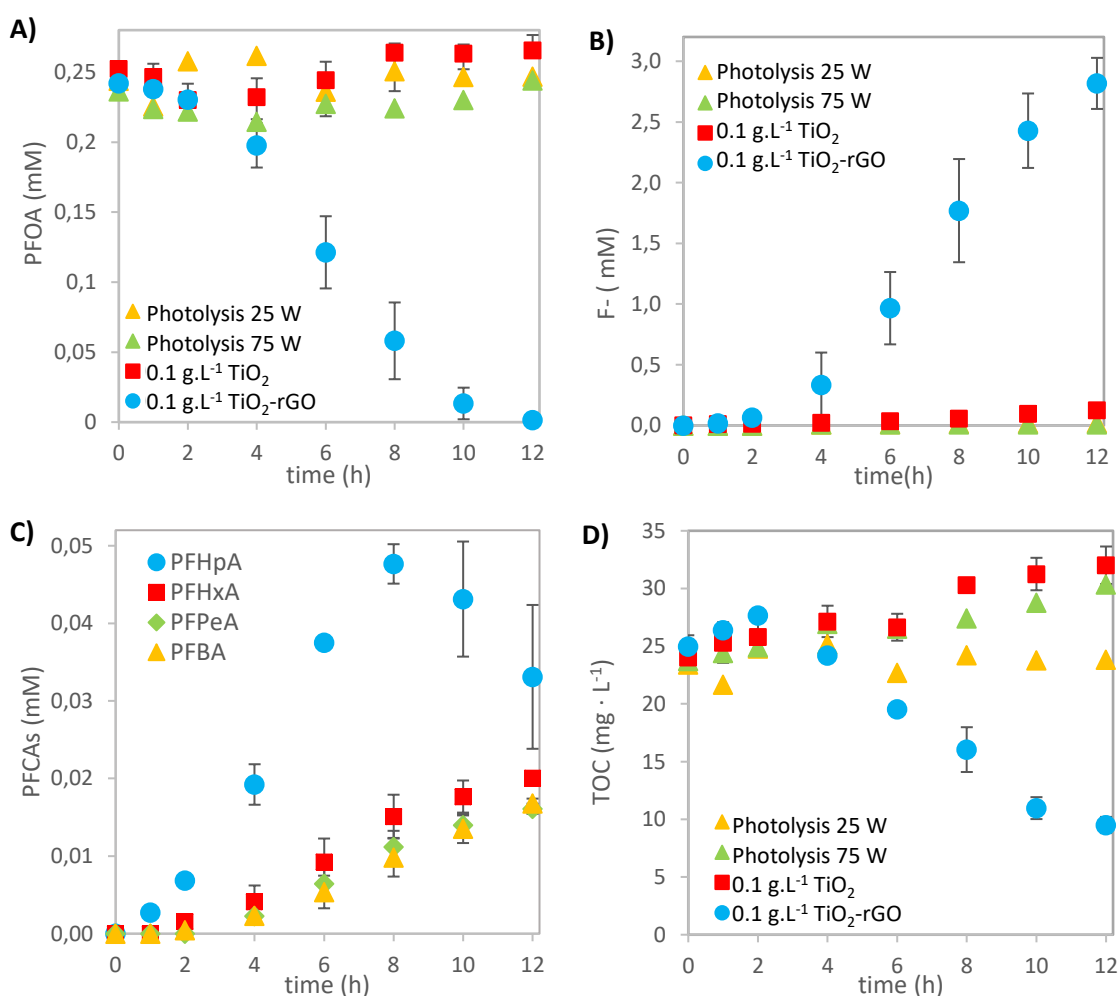


Figure 8. (A) PFOA degradation, (B) Fluoride release, (C) PFCAs generation (during TiO_2 -rGO photocatalytic treatment) and (D) TOC removal, under different conditions, in a LEDs lamp reactor with an initial 0.24 mM PFOA concentration.

The evolution of PFOA concentrations under the different experimental conditions are depicted in Figure 8(A). Firstly, it can be observed that there was no appreciable disappearance of PFOA by photolysis either at 25W or 75W of the light source power, after 12h of treatment. A possible reason is that PFOA molecules mainly absorb light with wavelengths that go from deep UV-region to 220nm (Hori et al, 2004; Cao et al,

2010) and the emissions wavelength of LEDs radiation was 365 nm. Therefore, UV-A LEDs light was unable to directly decompose PFOA molecule. Similarly, photocatalysis using TiO₂ did not degrade PFOA, in accordance with previously reported studies (Ab Aziz et al, 2016; Gómez-Ruiz et al, 2018; Estrellan et al, 2010; Sansotera et al, 2014; Li et al, 2016).

On the contrary, a significant PFOA elimination was observed when using TiO₂-rGO composite as catalyst, achieving 99 ± 1 % after 12h of irradiation. This high effectiveness of TiO₂-rGO composite for the degradation of PFOA, can be attributed to several reasons:

- i) Firstly, photo-generated electrons of TiO₂ particles under UV irradiation can be transferred to the graphene layer (rGO) due to its excellent electrical properties, acting as an electron-trap. (Wang et al, 2013). This mechanism further decreases the high electron/hole recombination of the TiO₂ semiconductor, and could promote the electron transfer from PFOA molecules which favours the initial degradation steps (Wang et al, 2017).
- ii) In addition, the structure and morphology of the composite may also have an important role during the photocatalytic treatment. Previous research (Gomez-Ruiz et al, 2018) revealed that TiO₂ nanoparticles exhibited a homogeneous distribution on the graphene nano-sheet that limited the TiO₂ trends to agglomerate when they are suspended in water during UV irradiation, which may provide more efficient use of the light.
- iii) Finally, the combination of rGO with TiO₂ might reduce the band gap energy (Li et al, 2013) which could provide TiO₂-rGO with the ability to adsorb visible light, facilitating a more efficient use of light than TiO₂ catalyst.

Besides, the released fluoride during the photocatalytic treatments is represented in Figure 8(B). Only using TiO₂-rGO catalyst, a significant increase of fluoride in the aqueous solution was observed, equal to 78 ± 6 % of the total fluorine that corresponds to 0.24 mM PFOA content. This demonstrated the effective cleavage of the C-F bonds in PFOA and in the rest of PFCAs intermediates.

Additionally, the fluorine mass balance was calculated and included in Figure 15, ANNEX II. At the beginning, the total content of fluorine was only assigned to the initial concentration of PFOA in the solution, but as the degradation process took place, the sum of the released fluoride and the fluorine contained in PFOA and intermediates were considered in the F balance. It is noteworthy that in the cases of direct photolysis and photocatalysis with TiO_2 , the calculated value of total F progressively increased with time, caused by an increment of the analyzed PFOA concentration during these experiments, showed in Figure 8(A). On the other hand, in the case of photocatalysis with TiO_2 -rGO composite, the total F mass balance remained nearly constant (3.6 mM) throughout the 12 hours of experiment, which means that all the released fluoride and the fluorine in PFOA and the rest of intermediates were measured properly.

Figure 8(C) shows the generation of shorter chain PFCA formed as intermediates when PFOA degraded. Shorter chain PFCA were observed in significant amounts only when using TiO_2 -rGO as photocatalyst. PFHpA was initially formed reaching higher generation rates, and after 8 hours of irradiation time, its concentration started to decrease giving the successive degradation products which were simultaneously formed and also degraded in shorter chain PFCA.

In addition, Figure 8(D) shows the progress of TOC removal to evaluate the PFOA mineralization. In the cases of photolysis and TiO_2 -mediated photocatalysis, TOC was not reduced during the irradiation time. On the contrary, using the composite TiO_2 -rGO, TOC showed a $62 \pm 4\%$ decrease, this percentage was not as large as the one of PFOA disappearance, because of the generation of intermediate PFCA products. The TOC values calculated from PFOA and intermediates concentrations were represented in Figure 16 in ANNEX II. In every experiment, values of calculated TOC were slightly lower than the measured ones, even for the initial value ($t=0$) when the degradation process had not started yet. For example, in photocatalysis with TiO_2 -rGO catalyst, 25 mg.L^{-1} were measured with the TOC-V CPH while 23.25 mg.L^{-1} were calculated. The gap between calculated and measured TOC in Figure 16 could be explained by the error and interferences in the TOC analytical method discussed in the previous section.

Focusing on PFOA degradation (Figure 8 (A)) by the composite TiO_2 -rGO photocatalyst, it is appreciable that there was an initial time delay before any PFOA degradation could

be observed. This delay, which was quantified in about two hours, can be also observed in the generation of fluoride degradation product. The presence of the time delay is not a common feature in photocatalytic systems and it was not observed in previous work on PFOA photocatalytic degradation with Hg lamp (Gómez-Ruiz et al, 2018), so several experiments were carried out in a trial to find an explanation of that special behavior.

3.3.1 Time delay study

Several hypothesis were figured out as origin of the time delay, and an experimental strategy was planned to check the validity of the propositions (Table 3).

Table 3. Figured out hypothesis and planned experimental strategies

<u>HYPOTHESIS</u>	<u>EXPERIMENTAL STRATEGY</u>
The light source needs time to heat up and arrive to steady state irradiation	Test 1: Measurement of the irradiance
Period of time needed for starting the generation hydroxyl radicals	Test 2: Measurement of the hydroxyl radicals
Influence of the adsorption of PFOA on the catalyst, before the reaction	Test 3: Two hours of PFOA + TiO ₂ -rGO mixture without UV light before switching on the experiment Test 4: TiO ₂ -rGO solution stirring under UV light for two hours before adding the PFOA solute
The catalyst needs activation	Test 5: Use of recovered TiO ₂ -rGO catalyst
There are problems of mass transfer in the reactor	Test 6: Use half of the catalyst's concentration (0.05 g.L ⁻¹) Test 7: Experiments using different initial PFOA concentrations

First of all, the irradiance produced by the light source was measured using a background PFOA solution (0.24 mM), with 0.1 g.L⁻¹ of TiO₂-rGO catalyst. Results obtained are displayed in Figure 9. Irradiance decreased with time, especially after the three first

hours of experiment. This decrease might be due to a small change of color in the solution produced by a partial reduction of the oxygen groups remaining in the TiO_2 -rGO catalyst caused by UV irradiation (Minella et al, 2015). In conclusion, these results did not give an explanation to the time delay, as in the first two hours of experiment the lamp irradiance was the highest one, which should have ended up in a higher photocatalytic efficiency.

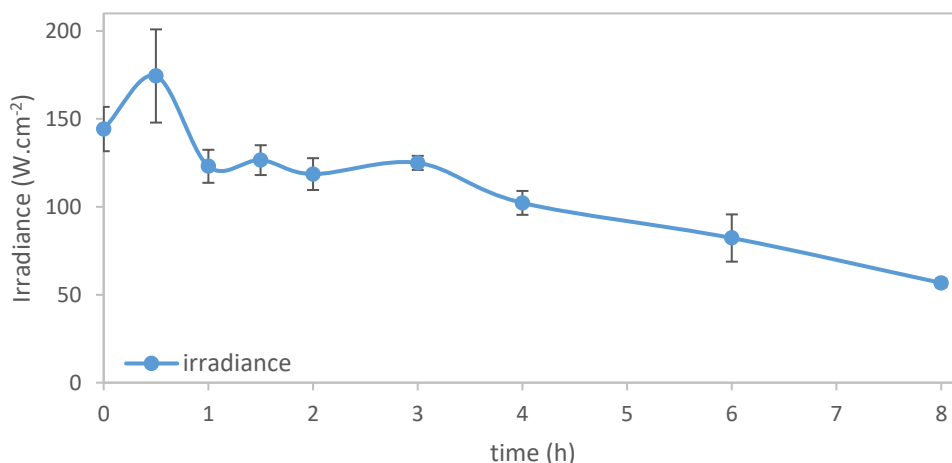


Figure 9. Irradiance emitted by LEDs lamp during 8 hours.

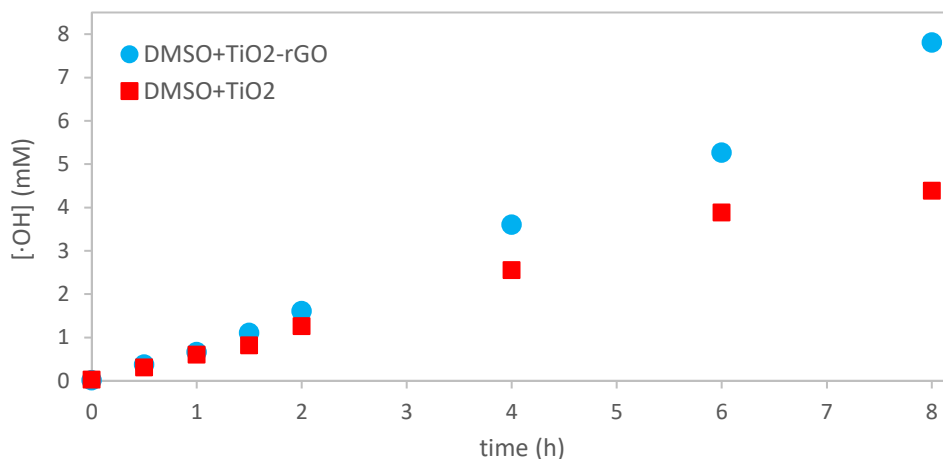


Figure 10. Generation of hydroxyl radicals applying photocatalysis with both $0.1 \text{ g} \cdot \text{L}^{-1} \text{TiO}_2$ -rGO and $0.1 \text{ g} \cdot \text{L}^{-1} \text{TiO}_2$, with an initial $0.25 \text{ mol} \cdot \text{L}^{-1} \text{DMSO}$ solution

The next test was to measure the rate of hydroxyl radicals generation by means of the DMSO transformation into formaldehyde, using TiO_2 and TiO_2 -rGO composite ($0.1 \text{ g} \cdot \text{L}^{-1}$). Figure 10 depicts the concentration of $\cdot\text{OH}$ with the irradiation time. The results showed similar $\cdot\text{OH}$ trends initially produced by both catalysts, and after 4 h, TiO_2 -rGO composite

seemed to generate higher content of these reactive species. The small difference between the data obtained in both cases was not enough to explain differences in results when using different catalysts. Additionally, there was a linear relation between $\cdot\text{OH}$ radicals and time, which is characteristic of low radiation intensities according to literature (Domínguez et al, 2016) and could not explain the initial time delay.

On the other hand, Test 3 to 6 were performed, applying in each one the conditions detailed in Table 3. The PFOA degradation is shown in Figure 11 (A). In all cases, similar trends of PFOA concentration with the irradiation time were obtained. All those changes had a minimal effect on PFOA removal. Additionally, fluoride release (Figure 11 (B)) did not showed significant differences among the different experiments, in good accordance with PFOA results.

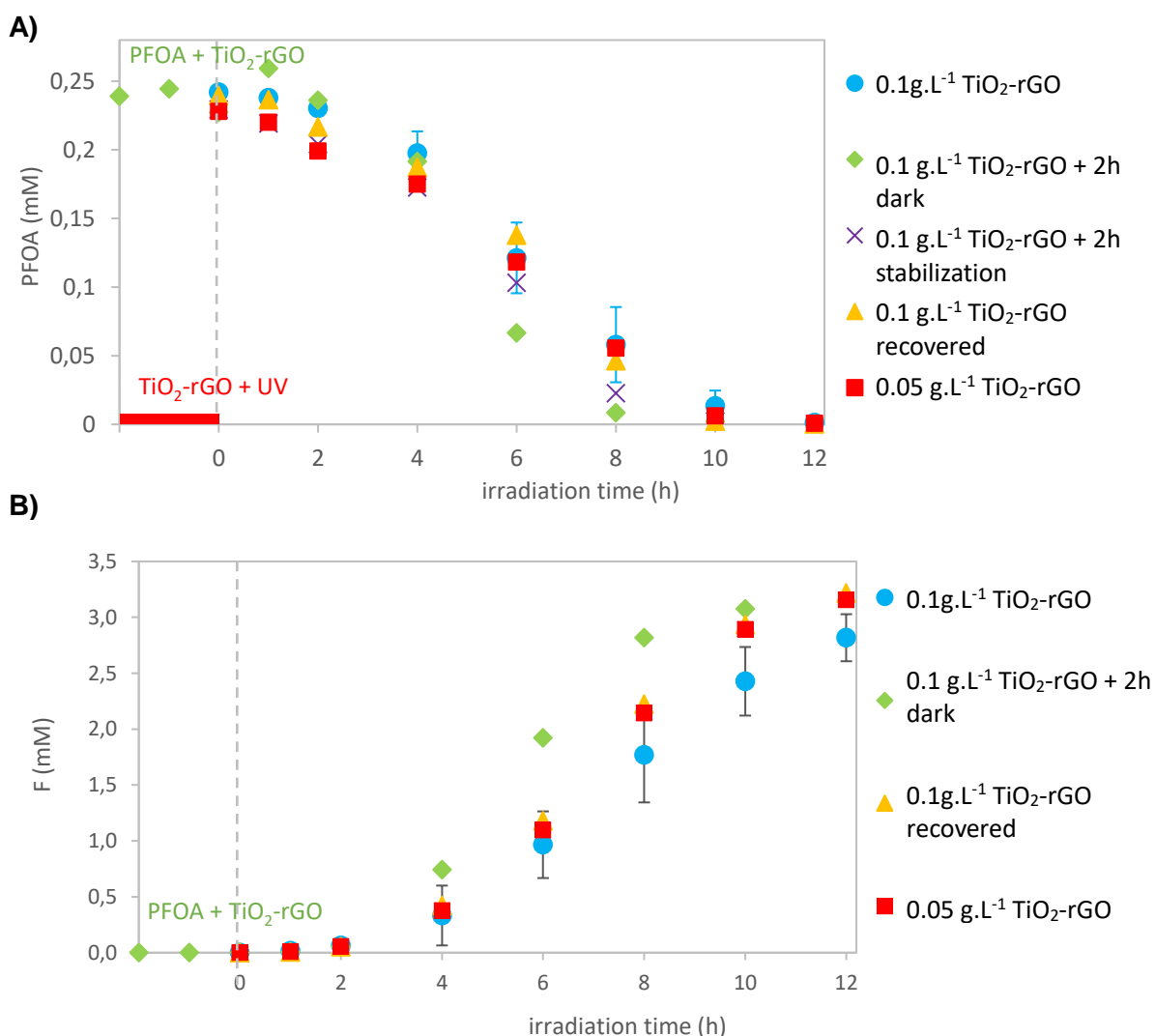


Figure 11. Progress of (A) PFOA removal and (B) fluoride release under different conditions, using the composite TiO₂-rGO catalyst in a LEDs lamp reactor with an initial 0.24 mM PFOA concentration. Power to LEDs lamp = 75 W.

Besides, intermediate PFCAs formation and PFOA mineralization were also measured and results have been included in Figures 17 and 18 in ANNEX III. Those results were again very similar to the ones obtained in the photocatalytic experiment of PFOA by means of $0.1 \text{ g}\cdot\text{L}^{-1}$ $\text{TiO}_2\text{-rGO}$ (blue circles), reaffirming the minimal effect of the proposed test on the PFOA removal rates obtained under UV irradiation.

Finally, the influence of the initial PFOA concentration on the photocatalytic process was studied. For this purpose, the initial concentration of PFOA in the aqueous solution was set at three values: 0.48 mM, 0.24 mM and 0.12 mM. All experiments were carried out twice in order to prove their reproducibility, so average values and deviations for PFOA, fluoride and TOC concentrations were calculated. Besides, the amount of catalyst used was $0.05 \text{ g}\cdot\text{L}^{-1}$ since it was observed that PFOA degradation had the same efficiency as for $0.1 \text{ g}\cdot\text{L}^{-1}$. In addition, one experiment using an initial 0.48 mM PFOA solution and $0.1 \text{ g}\cdot\text{L}^{-1}$ of $\text{TiO}_2\text{-rGO}$ catalyst was also performed for comparison.

Figure 12 shows the progress of PFOA concentration (A) and released fluoride (B) during irradiation time in the photocatalytic experiments using $\text{TiO}_2\text{-rGO}$ and the different initial PFOA concentrations. Last points of PFOA concentration (8h to 12h) for the experiment with a 0.48 mM initial PFOA concentration and $0.05 \text{ g}\cdot\text{L}^{-1}$ $\text{TiO}_2\text{-rGO}$ catalyst, were below the limits of quantification.

The significant influence of the initial concentration of PFOA in the photocatalytic process can be observed. Higher initial PFOA concentrations (0.48 mM and 0.24 mM) favoured greater and similar removal rates, while at the lowest initial concentration (0.12 mM) PFOA degradation was practically nulled. In addition, it seems that at 0.48 mM PFOA initial concentration, the degradation was slightly faster with $0.1 \text{ g}\cdot\text{L}^{-1}$ than with $0.05 \text{ g}\cdot\text{L}^{-1}$ of $\text{TiO}_2\text{-rGO}$ catalyst concentration. This behavior demonstrated the idea of the need of PFOA interaction with the catalyst during the UV irradiation to initiate the photocatalytic degradation of PFOA.

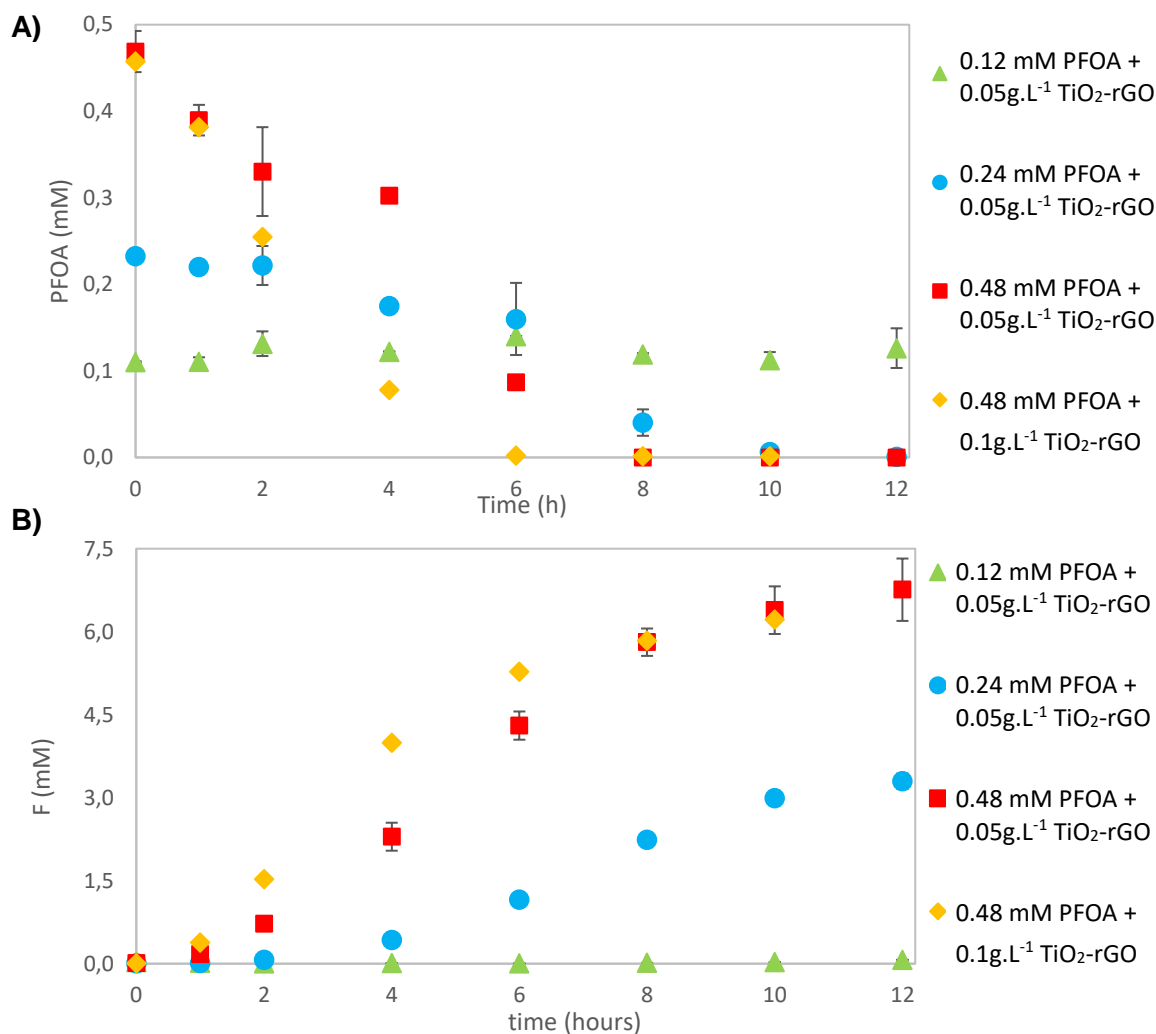


Figure 12. (A) PFOA degradation and (B) Fluoride release in photocatalytic experiments using TiO₂-rGO with different initial PFOA concentrations in a LEDs lamp reactor. Power to LEDS lamp = 75 W.

Although PFOA is a surfactant that can form micelles, this property does not explain these results, since all the experiments were carried out below the micellar critical concentration calculated for PFOA, which is equal to 7.8 mM at 25°C (Sansotera et al, 2015).

Similar to PFOA trends, the fluoride content progressively increased with time only in the cases of higher initial PFOA concentrations. However, no fluoride release could be observed during the photocatalytic treatment of 0.12 mM PFOA solutions.

Moreover, the mineralization of PFOA was monitored, as represented in Figure 19 in ANNEX III. It can be observed that there is a high PFOA mineralization for higher

concentrations while it is negligible for the process with 0.12 mM initial PFOA, reinforcing PFOA and fluorine results.

Finally, further research will be developed to explain the mechanism of interaction between TiO₂-rGO and PFOA to consequently promote the contaminant degradation.

4. CONCLUSIONS

This final degree project aims at studying the photocatalytic degradation of perfluorooctanoic acid (PFOA) using a TiO₂-rGO catalyst synthesized in the laboratory applying a hydrothermal method (Ribao et al, 2017; Li et al, 2013). For this purpose, two different experimental systems were used.

Firstly, the photocatalytic experiments carried out in a medium pressure mercury lamp reactor (200-600 nm) resulted in similar PFOA removal rates by means of direct photolysis and photocatalysis with the use of TiO₂ and the prepared TiO₂-rGO composite. However, these findings were different compared to the previous reported work under similar experimental conditions (Gómez-Ruiz et al, 2018). These results likely showed an instability of the medium pressure Hg lamp.

For the first time in PFOA degradation studied, the next experimental system consisted of a light emitting diode (LEDs) lamp reactor (365 nm). After 12 hours applying direct photolysis and photocatalysis with TiO₂ to a 0.24 mM PFOA solution, no degradation of the contaminant was observed. On the contrary, using 0.1 g.L⁻¹ of TiO₂-rGO catalyst, a 99 ± 1 % PFOA removal was achieved, proving the high photocatalytic activity of the composite TiO₂-rGO for PFOA degradation. Additionally, these results represented a huge improvement with respect to the previous results obtained with the conventional Hg lamp for the same composite. It is also remarkable that in photocatalysis with TiO₂-rGO with the LEDs lamp reactor, there was an initial time delay before any PFOA degradation could be observed, which was quantified in about two hours. Several tests were carried out in order to associate the delay with factors such as irradiation energy, hydroxyl radicals generation, PFOA adsorption, TiO₂-rGO catalyst activation under UV light or limitations of mass transfer. Only the tests carried out to study the influence of PFOA initial concentration on the photocatalytic process showed a notable effect, in

which the higher the initial PFOA concentration was (0.24 and 0.48 mM), the faster the degradation took place. This could indicate the necessity of PFOA and catalyst interaction under UV-light, which seems to be favored by increasing the initial PFOA concentration. Finally, further investigation will be carried out in order to understand the mechanism of interaction between TiO₂-rGO and PFOA that enables promoting the contaminant degradation.

To sum up, photocatalytic degradation by means of TiO₂-rGO in the LEDs system is a promising technology for the elimination of PFASs recalcitrant compounds in water, due to the high photoactivity exhibited by the prepared TiO₂-rGO composite. In addition, LEDs appear as an alternative to conventional light sources, improving their lifetime, efficiency and sustainability.

5. REFERENCES

Ab Aziz, N., Palaniandy, P., Aziz, H. A., Dahlan, I. *Review of the mechanism and operational factors influencing the degradation process of contaminants in heterogeneous photocatalysis*. J. Chem. Res ,vol. 40, pp.704–712. (2016).

Appleman, T.D., Higgins, C.P., Quiñones, O., Vanderford, B.J., Kolstad, C., Zeigler-Holady, J.C., Dickenson, E. *Treatment of poly- and perfluoroalkyl substances in U.S. full-scale water treatment systems*. *Water Res.*, Vol. 51, pp.246 – 255. (2014).

Bartlett, S.A., Davis, K.L. *Evaluating PFAS cross contamination issues*. *Remediation Journal*, vol. 28, magazine number 2. (2018).

Cao, M.H., Wang, B.B., Yu, H.S., Wang, L.L., Yuan, S.H., Chen, J. *Photochemical decomposition of perfluorooctanoic acid in aqueous periodate with VUV and UV light irradiation*. *J. Hazard. Mater.*, vol.179, pp.1143–1146. (2010).

Domínguez S., Rivero M.J., Gomez P., Ibañez R., Ortiz I. *Kinetic modeling and energy evaluation of sodium dodecylbenzenesulfonate photocatalytic degradation in a new LED reactor*. (2016).

Estrellan, C.R., Salim, C., Hinode, H. *Photocatalytic decomposition of perfluorooctanoic acid by iron and niobium co-doped titanium dioxide*. J. Hazard. Mater, vol.179, pp.79–83. (2010).

Flores, C., Ventura, F., Martin-Alonso, J., Caixach, J. *Occurrence of perfluorooctane sulfonate (PFOS) and perfluorooctanoate (PFOA) in N.E. Spanish surface waters and their removal in a drinking water treatment plant that combines conventional and advanced treatments in parallel lines*. Sci. Total Environ., pp. 461-462, 618-626 (2013).

Fuertes, I., Gómez-Lavín, S., Elizalde, M.P., Urtiaga, A. *Perfluorinated alkyl substances (PFASs) in northern Spain municipal solid waste landfill leachates*. Chemosphere, Vol. 168, pp. 399-407. (2017).

Fujii, S., Polprasert, C., Tanaka, S., Lien, N., Qiu, Y. *New POPs in the water environment: distribution, bioaccumulation and treatment of perfluorinated compounds – a review paper*. J. Water. Supply. Res. T., Vol. 56, pp. 313-326 (2007).

Gómez-Ruiz, B., Gómez-Lavín, S., Diban, N., Boiteux, V., Colin, A., Dauchy, X., Urtiaga, A. *Efficient electrochemical degradation of poly- and perfluoroalkyl substances (PFASs) from the effluents of an industrial wastewater treatment plant*. Chemical engineering Journal, Vol. 322, pp.196-204. (2017).

Gómez-Ruiz, B., Ribao P., Diban N., Rivero M.J., Ortiz I., Urtiaga I. *Photocatalytic degradation and mineralization of perfluorooctanoic acid (PFOA) using a composite TiO₂-rGO catalyst*. Journal of Hazardous Materials, Vol.344, pp.950-957. (2018).

Haque, M.M., Bahnemann, D., Muneer, M. *Photocatalytic Degradation of Organic Pollutants: Mechanisms and Kinetics, Organic Pollutants Ten Years after the Stockholm Convention - Environmental and Analytical Update*. (2012).

Hazetova, K., Urtiaga, A. *Preliminary study of perfluorooctanoic acid decomposition by heterogeneous photocatalysis*. (2015).

Hori, H., Hayakawa, E., Einaga, H., Kutsuna, S., Koike, K., Ibusuki, T. Kiatagawa, H., Arakawa, R. *Decomposition of environmentally persistent perfluorooctanoic acid in*

water by photochemical approaches. Environ. Sci. Technol., Vol.38, pp.6118–6124. (2004)

Hradkova, P., Poustka, J., Hlouškova, V., Pulkrabova, J., Tomaniova, M., Hajšlova, J. *Perfluorinated compounds: occurrence of emerging food contaminants in canned fish and seafood products*. Czech J. Food Sci., vol.28, pp.333-342 (2010).

Hummers W.S., Offeman R.E. *Preparation of Graphitic Oxide*. J. Am. Chem. Soc. Vol.80 pp.1339–1339. (1958).

Lee, J.W., Lee, J.W., Kim, K., Shin, Y.J, Kim, J., Kim, S., Kim, H., Kim, P., Park, K. *PFOA-induced metabolism disturbance and multi-generational reproductive toxicity in *Oryzias latipes**. Journal of hazardous materials, vol. 340. (2017).

Li, J., Zhou, S. L., Hong, G., Chang, C. *Hydrothermal preparation of P25-graphene composite with enhanced adsorption and photocatalytic degradation of dyes*. Chem. Eng. J. pp. 486-491 (2013b).

Li, M., Yu, Z., Liu, Q., Sun, L., Huang, W. *Photocatalytic decomposition of perfluorooctanoic acid by noble metallic nanoparticles modified TiO_2* , Chem. Eng. J., vol.286, pp.232–238. (2016).

Nakata, K., Fujishima, A. *TiO_2 photocatalysis: Design and applications*. Journal of photochemistry and photobiology C: photochemistry reviews, vol. 13, issue 3. Pp. 169-189 (Sept. 2012).

Pei, F., Liu, Y., Zhang, L., Wang, S., Xu, S., Cao, S. *TiO_2 nanocomposite with reduced graphene oxide through facile blending and its photocatalytic behaviour for hydrogen evolution*. Mater. Res. Bull. pp. 2824-2831 (2013).

Pistocchi, A., Loos, R. *A map of European emissions and concentrations of PFOS and PFOA*. Environ. Sci. Technol., vol. 43, pp. 9237-9244. (2009).

Post, G.B., Cohn, P.D., Cooper, K.R. *Perfluorooctanoic acid (PFOA), an emerging drinking water contaminant: A critical review of recent literature*. Environ. Res., vol. 116, pp. 93–117. (2012).

Prevedouros, K; Cousins, I; Buck, R; Korzeniowski, S. *Sources, fate and transport of perfluorocarboxylates*. Environmental Science and Technology, vol. 40, pp.32-44. (2006).

Ribao, P., Rivero, M., Ortiz, I. *Enhanced photocatalytic activity using GO/TiO₂ catalyst for the removal of DCA solutions*. Environmental science and pollution research. (2017).

Rivero, M.J., Ribao, P., Domínguez, S., Ortiz, I. *Influence of the Synthesis Method on the Photocatalytic activity of Graphene Oxide/Titanium Dioxide Composites*. 4th European Conference on Environmental Applications of Advanced Oxidation Processes Athens (Greece), pp. 21-24. (October, 2015).

Sansotera, M., Persico, F., Pirola, C., Navarrini, W., Di Michele, A., Bianchi, C.L. *Decomposition of perfluorooctanoic acid photocatalyzed by titanium dioxide: Chemical modification of the catalyst surface induced by fluoride ions*, Appl. Catal. B Environ. 148–149. 29–35. (2014).

Sansotera, M., Persico, F., Rizzi, V., Panzeri, W., Pirola, C., Bianchi, C.L., Mele, A., Navarrini, W. *The effect of oxygen in the photocatalytic oxidation pathways of perfluorooctanoic acid*. Journal of Fluorine Chemistry (2015).

Soriano, A., Gorri, D., Urtiaga, A. *Efficient treatment of perfluorohexanoic acid by nanofiltration followed by electrochemical degradation of the NF concentrate*. Water research, vol.112, pp. 147-156. (2017).

Squadrone, S., Ciccotelli, V., Prearo, M., Favaro, L., Scanzio, T., Fogliani, C., Abete, M.C. *Perfluorooctane sulfonate (PFOS) and perfluorooctanoic acid (PFOA): emerging contaminants of increasing concern in fish from lake Varese, Italy*. Environmental monitoring and assessment, vol.187, magazine number 7. (2015).

Tai, C., Peng, J.F., Liu, J.F., Jiang, G.B., Zou, H. *Determination of hydroxyl radicals in advanced oxidation processes with dimethyl sulfoxide trapping and liquid chromatography*. Anal Chim Acta, vol.527, pp. 73–80. (2004).

Urutiaga, A., Fernández González, C., Gámez Lavín, S., Ortiz, I. 2015. *Kinetics of the electrochemical mineralization of perfluorooctanoic acid on ultrananocrystalline boron doped conductive diamond electrodes*. *Chemosphere*, vol.129, pp.20-26 (2015)

United States Environmental protection Agency: U.S. E.P.A *Drinking water health advisory for perfluorooctanoic Acid (PFOA)*. (May 2016).

Wang, P., Wang, J., Wang, X., Yu, H., Yu, J., Lei, M., Wang, Y. One-step synthesis of easy-recycling TiO₂-rGO nanocomposite photocatalysts with enhanced photocatalytic activity. *Appl. Catal. B-Environ.*, 132-133, 452-459 (2013).

Wang, S., Yang, Q., Chen, F., Sun, J., Luo, K., Yao, F., Wang, X., Wang, D., Li, X., Zeng, G. *Photocatalytic degradation of perfluorooctanoic acid and perfluorooctane sulfonate in water: a critical review*. *Chemical engineering Journal*, vol.328, pp.927-942. (Nov. 2017).

Zhang, Y., Pan, C. *TiO₂/graphene composite from thermal reaction of graphene oxide and its photocatalytic activity in visible light*. *J. Environ. Sci.*, vol.46, Pp.2622-2626 (2011).

6. ANNEXES

6.1 ANNEX I: Medium pressure Hg lamp reactor

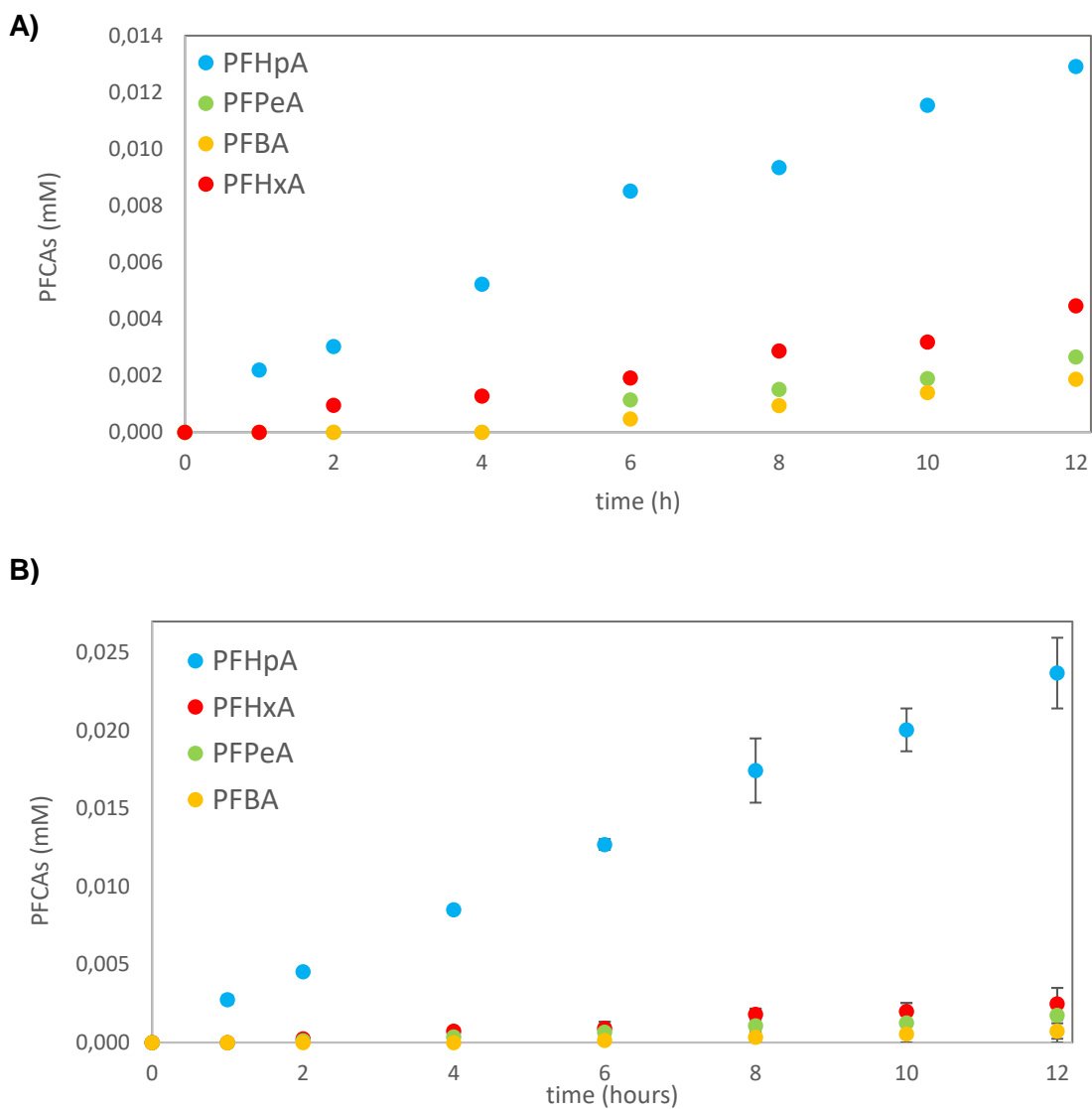


Figure 13. PFCAs formed in a medium pressure Hg lamp reactor with a 0.24mM Initial PFOA solution for (A) TiO_2 catalyst and (B) TiO_2 -rGO

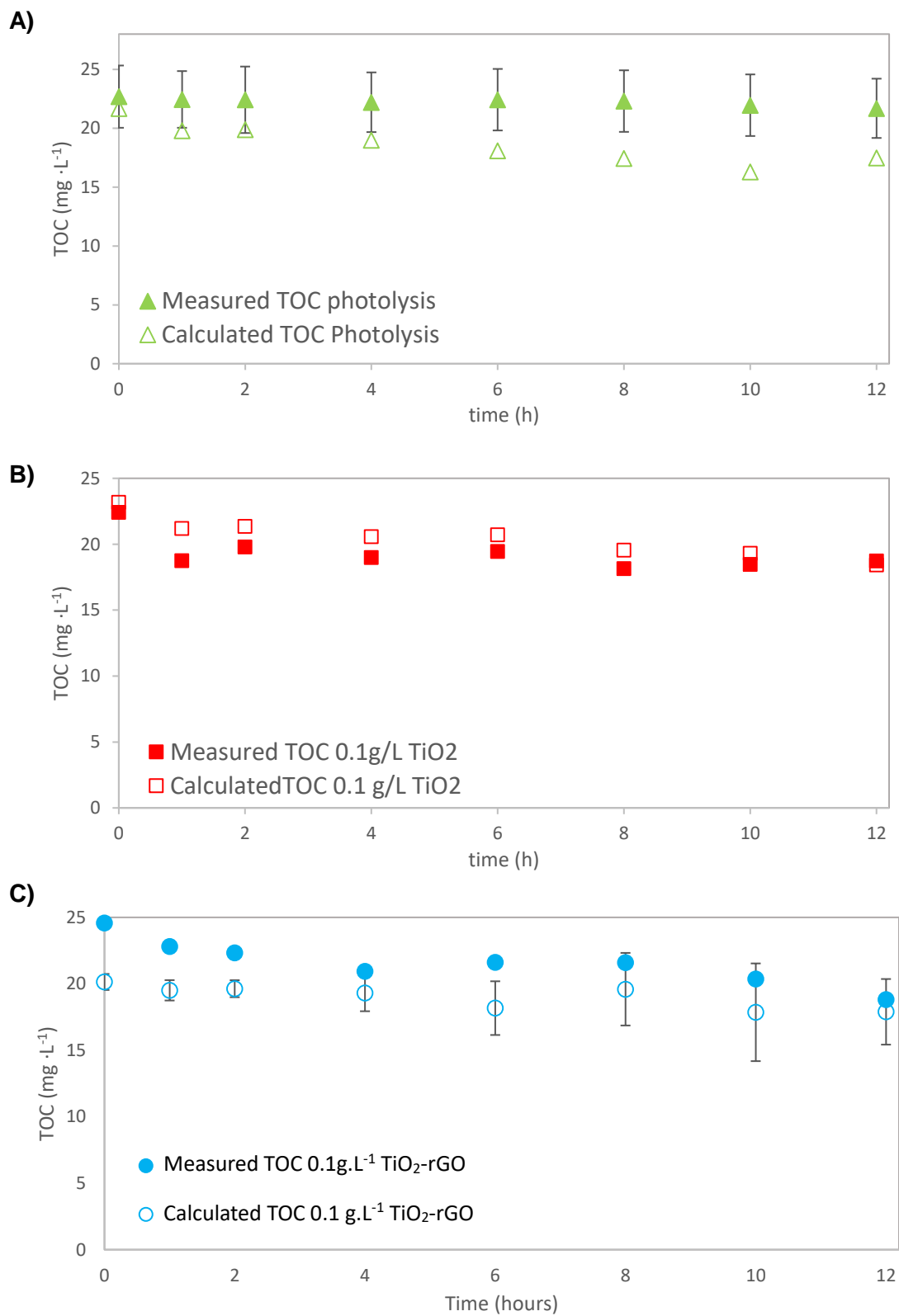


Figure 14. Calculated and Measured TOC data in a medium pressure Hg lamp reactor with a 0.24 mM initial PFOA solution for (A) direct photolysis (B) photocatalysis with TiO₂ and (C) photocatalysis with TiO₂-rGO

3.4 ANNEX II: LEDs lamp reactor

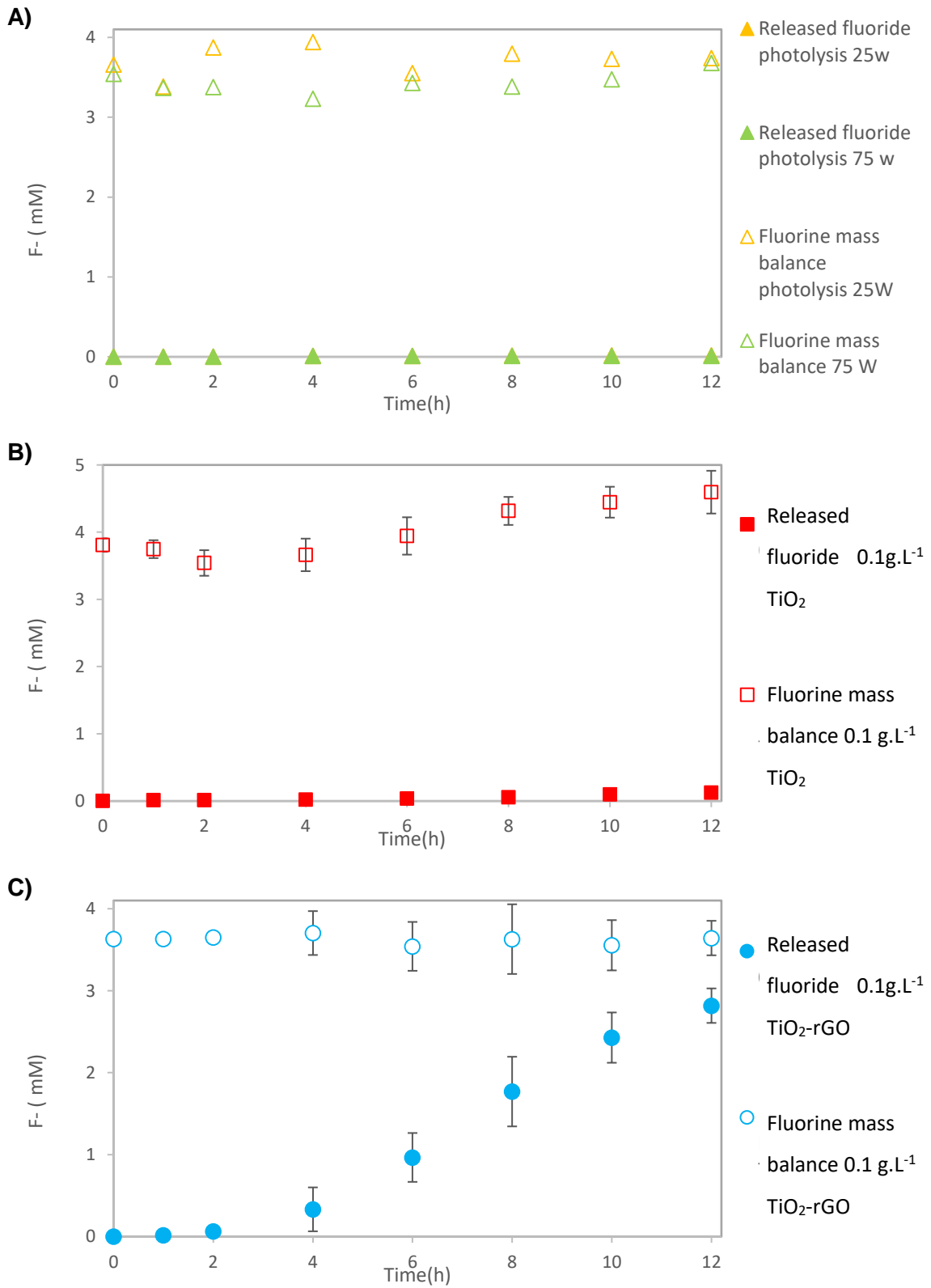


Figure 15. Fluorine mass balance and fluoride release in a LEDs lamp reactor reactor with a 0.24 mM initial PFOA solution for (A) direct photolysis (B) photocatalysis with TiO₂ and (C) photocatalysis with TiO₂-rGO

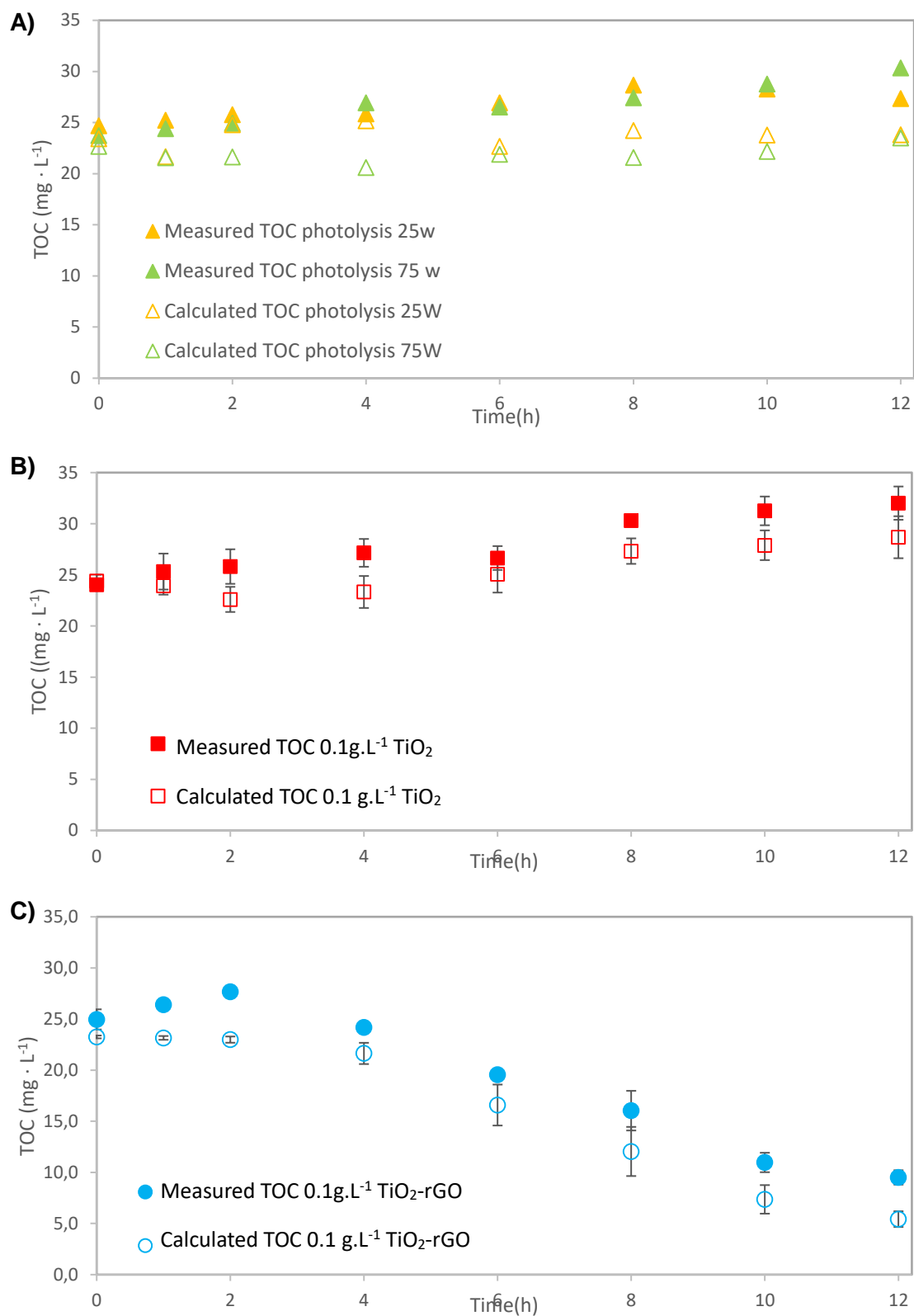


Figure 16. Calculated and measured TOC in a LEDs lamp reactor reactor with a 0.24 mM initial PFOA solution for (A) direct photolysis (B) photocatalysis with TiO₂ and (C) photocatalysis with TiO₂-rGO

3.5 ANNEX III: Time delay study

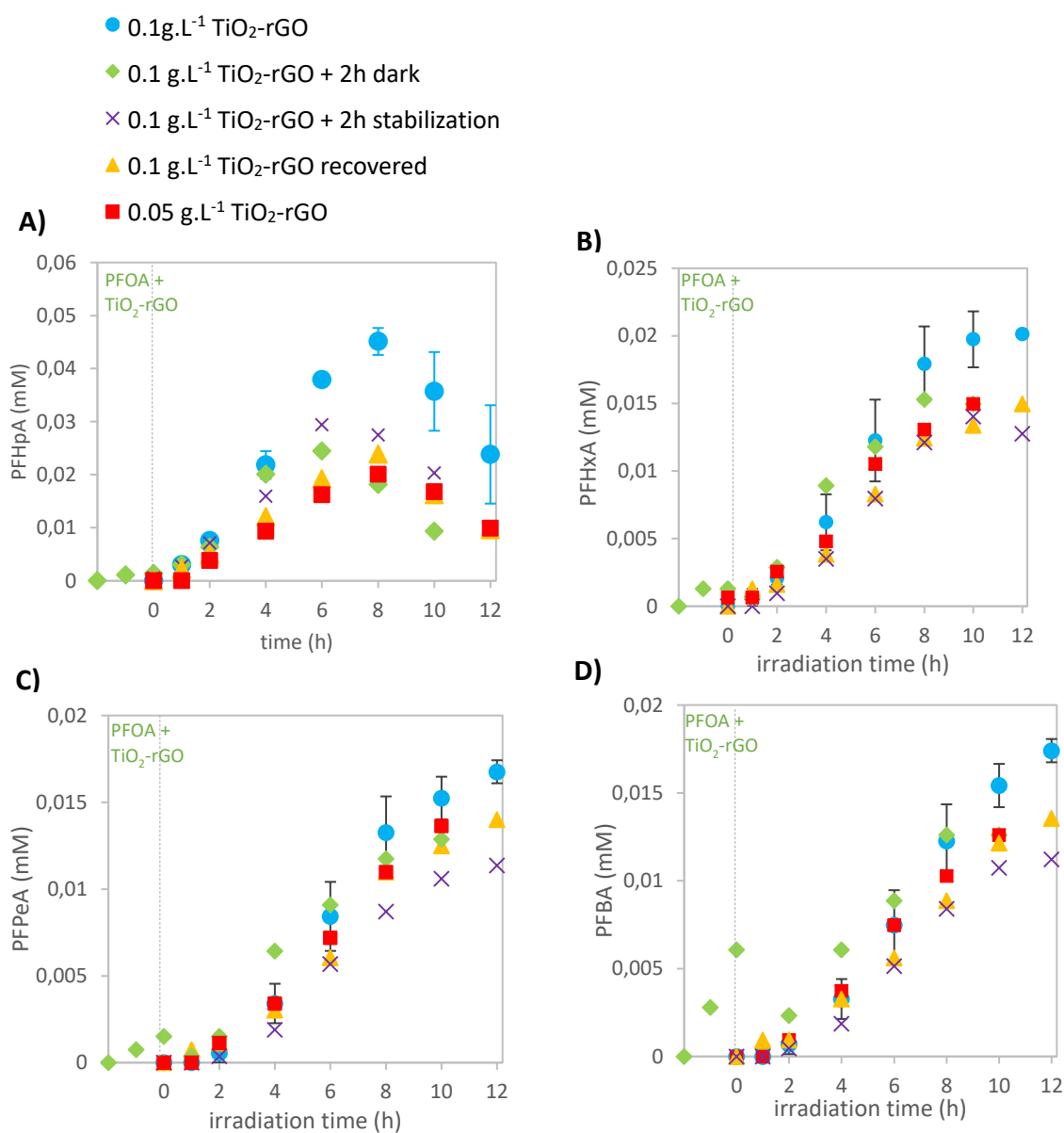


Figure 17. Formation of (A) PFHpA, (B) PFPxA, (C) PFPeA and (D) PFBA in photocatalytic experiments, under different conditions, using TiO₂-rGO with a 0.24mM initial PFOA concentration in a LEDs lamp reactor. Power to the LEDs lamp = 75W.

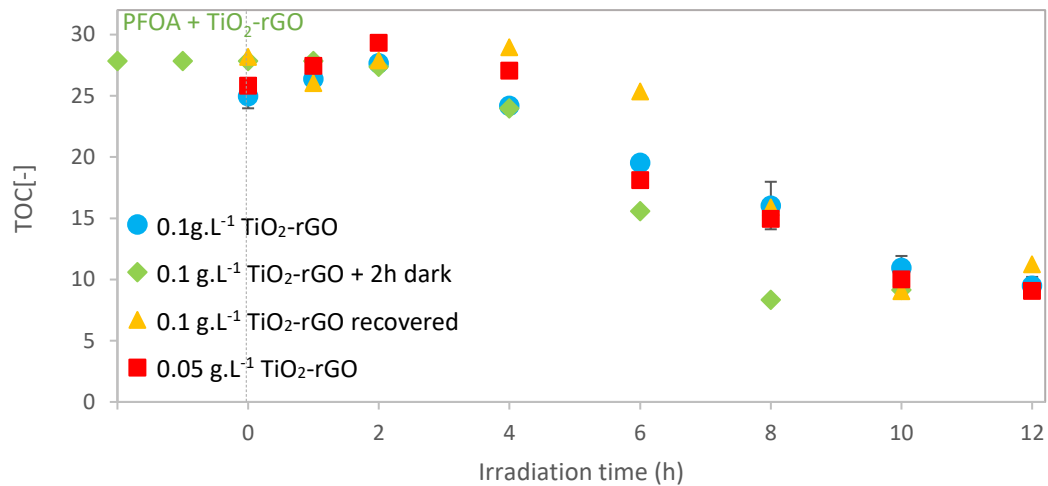


Figure 18. TOC trends in photocatalytic experiments, under different conditions, using TiO₂-rGO with a 0.24mM initial PFOA concentration in a LEDs lamp reactor. Power to the LEDs lamp = 75W.

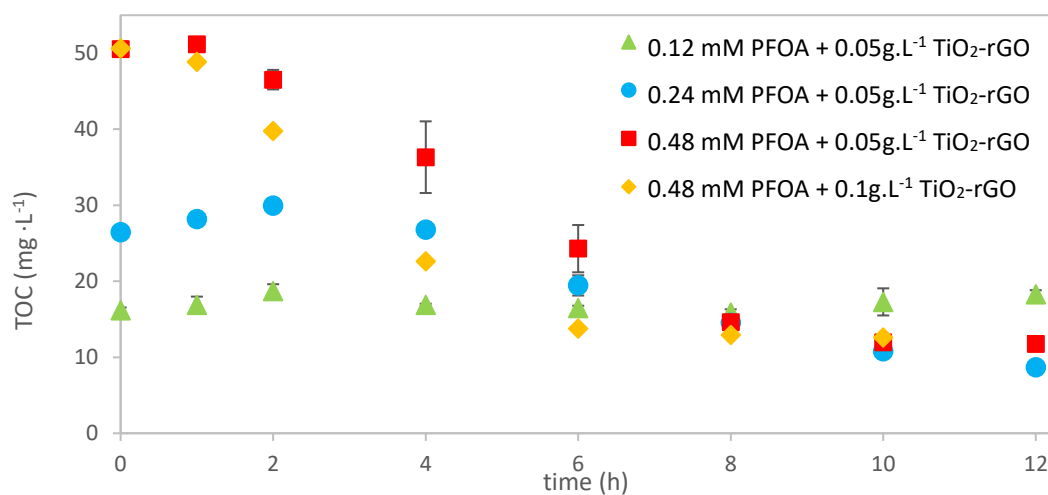


Figure 19. TOC trends in photocatalytic experiments, under different conditions, using TiO₂-rGO in a LEDs lamp reactor. Power to the LEDs lamp = 75W.